Global ocean re-analyses for climate applications

Simona Masina[1,2*], Pierluigi Di Pietro[2], Andrea Storto[1] and Antonio Navarra[1,2]

[1]Centro Euro-Mediterraneo per i Cambiamenti Climatici, Bologna, Italy

[2] Istituto Nazionale di Geofisica e Vulcanologia, Bologna, Italy

*Corresponding author: Phone: +39-051-3782620. Fax: +39-051-3782655

Keywords: data assimilation, global ocean, numerical models, climate

Abstract

One of the main objectives of the global ocean modelling activities at Centro Euro-Mediterraneo per i Cambiamenti Climatici (CMCC) is the production of global ocean re-analyses over multidecadal periods to reconstruct the state of the ocean and the large scale circulation over the recent past. The re-analyses are used for climate applications and for the assessment of the benefits of assimilating ocean observations on seasonal and longer predictions.

Here we present the main characteristics of an Optimal Interpolation based assimilation system used to produce a set of global ocean re-analyses validated against a set of high quality in situ observations and independent data. Differences among the experiments of the set are analyzed in terms of improvements in the method used to assimilate the data and the quality of observations themselves. For example, the integrated ocean heat content, which can be taken as an indicator of climate changes, is examined to detect possible sources of uncertainty of its long-term changes. Global and basin scale upper ocean heat content exhibits warming trends over the last few decades that still depend in a significant way on the assimilated observations and the formulation of the background covariances. However, all the re-analyses show a global warming trend of the oceanic uppermost 700 m over the last five decades that falls within the range of the most recent observation-based estimates. The largest discrepancies between our estimates and observational based ones are confined in the upwelling regions of the Pacific and Atlantic Oceans. Finally, the results show that the climatological heat and salt transports as a function of latitude also fall within the range of the estimates based on observations and atmospheric re-analyses.

1. Introduction

It is now internationally recognized that the ocean is a crucial component of the Earth's climate system and a driver of many important climate processes at a range of time and geographical scales. The estimation of the present and past three-dimensional state of the ocean is an essential target in the context of both climate variability assessments and predictability purposes such as the production of ocean initial conditions for seasonal and longer time-scale climate forecasts. However, in spite of the most recent efforts aimed at extending the available observational dataset and introducing new ones, the oceans remain seriously under-sampled and time series are often of limited usefulness for general conclusions related to climate change issues due to the short periods of coverage and sparse geographical distributions. On the other hand, considerable advancements have been made in the development of ocean data assimilation techniques over the course of the past few decades, and a number of global ocean data assimilation (ODA) systems have been developed to estimate the time-evolving, three-dimensional state of ocean circulation. Results are especially useful for analyzing unobserved quantities, such as the meridional overturning circulation and the oceanic heat transport, important elements for monitoring climate variations.

Today, several global ocean data assimilation products are available and can be used for several purposes as climate applications and initialization problems. Assimilation schemes range from simple and computationally efficient (e.g., optimal interpolation) to sophisticated and computationally intensive (e.g., adjoint, Kalman filters, and smoothers).

The number of studies that utilize the products from these systems to investigate various aspects of ocean circulation and climate variability is increasing. For instance, ODA products have been

applied to study a wide range of topics in physical oceanography and climate research, like the nature of sea level variability (e.g., Carton et al. 2005, Köhl and Stammer 2008), mixed-layer heat balance (e.g., Drbohlav et al., 2007, Halkides and Lee, 2009), trend and variability of the upper-ocean (Masina et al., 2004, Carton and Santorelli, 2008). Pierce et al. (2000) and Pohlmann et al. (2009) show applications of ODA products for initializing coupled climate models and many examples exist about their beneficial impact on climate forecasts at the seasonal time scale (among the most recent Balmaseda et al., 2007, Zheng et al., 2007, Hackert et al., 2007, Alessandri et al., 2010, Balmaseda et al., 2010). Similarly to the common practice with atmospheric re-analyses, the recent availability of global ocean re-analyses has allowed to use them as a reference for the evaluation of model performances. For example, ocean re-analyses have been used to estimate coupled model biases in simulating the thermal vertical structure in the Equatorial Pacific (Cherchi et al., 2008) and the ENSO dynamics (Capotondi et al., 2006, Navarra et al. 2008). Examples and applications of global ocean re-analyses from different institutions are provided by Lee et al. (2010a) and Stammer et al. (2010). As part of this effort, a large suite of indices and diagnostic quantities obtained from various ODA products are compared and evaluated using observations when available. For example Lee et al., (2010b) provides an overview of the current quality of the global ODA products in their ability to reproduce one of the critical components of the global thermohaline circulation, the Indonesian through flow.

This work is intended to provide the description of a set of global ocean re-analysis produced at our institute with the CMCC-INGV Global Ocean Data Assimilation System (CIGODAS) over the last few years and an example of a possible validation strategy with the purpose to show the applicability of these products for studies of climate change and variability.

In the following Section we describe the assimilation system with its three components: the dynamical model, the assimilation scheme and the various releases of the observed temperature and salinity profiles used. In Section 3 the skill of the re-analyses in representing the ocean state has been evaluated against observed data among which several are independent data sets. Some possible applications of the re-analyses in particular for climate applications are presented and discussed in Section 4. Finally the last Section includes a summary and some final remarks on the system and some of the most recent on-going developments.

2. The Global Ocean Data Assimilation System

The CIGODAS is composed of the Ocean General Circulation Model (OGCM) OPA 8.2 (Madec et al., 1999) in the ORCA2 global configuration (horizontal resolution of 2° longitude x 2°cos(φ) latitude), and an Optimal Interpolation (OI) scheme based on the System for Ocean Forecasting and Analysis (SOFA) assimilation software (De Mey and Benkiran, 2002). The SOFA code has been originally modified to be implemented to the global ocean for the assimilation of temperature and salinity (Bellucci et al. , 2007).

2.1 Ocean model and the CTRL experiment

In all the re-analyses that we produced, the free-surface version of the ocean model OPA 8.2 (Madec et al., 1999) is spun up with ERA-40 (Uppala et al. 2005) derived climatological fluxes of momentum, heat, and freshwater for five years , starting from a motionless ocean, and Levitus hydrographical initial conditions (Levitus et al., 1998). A spin up that covers the period from 1953 to 1957 is followed by a simulation forced with daily ERA-40 fluxes from January 1958 to December 1961. Sea surface temperatures are restored to an ERA-40 climatological year (1971-

2000) with a Newtonian damping heat flux of 200 $W \cdot m^{-2} \cdot K^{-1}$,corresponding to a restoring time scale of about 12 days (assuming a mixed layer thickness of 50 m). A weaker relaxation to Levitus et al. (1998) temperature and salinity climatology along the whole water column is also applied, with a 3-yr damping time scale.

The ocean state at the end of 1961 provides the initial conditions for the interannually forced run (CTRL, see Table 1), starting on 1st January 1962. The integrations are performed by using the same forcings and restoring parameters adopted to generate the 1958-61 non-climatological spin up, except for the sea surface temperatures that are relaxed to monthly HadISST data (Rayner et al., 2003) up to Dec 1981, then to Reynolds temperatures (Reynolds, 1988) from Jan 1982 to Aug 2002, linearly interpolated to daily values. Operational ECMWF SST fields are then used, starting from September 2002 onwards.

During the model integration, a daily adjustment is applied to the global sea surface height, aimed at removing a drift associated with the nonzero residual of the globally averaged freshwater fluxes. An improved version of ERA-40 freshwater fluxes, correcting a bias in the precipitation (Troccoli and Källberg 2004) is used. From January 2002 onwards operational ECMWF fields are used as forcing fields (wind stress, heat and freshwater fluxes).

In order to prevent the onset of a numerical instability in the Southern Ocean, off the Antarctic coast, a full-depth relaxation to Levitus temperature and salinity climatology is applied poleward of 60°N/60°S, with a gradual reduction of the restoring time scale from 3 yr to 50 days occurring in the 60°-70°N (S) latitude belt. The restoring time scale is 50 days at the top level, gradually increasing to 1 yr at the bottom.

2.2 Assimilation scheme

The assimilation of observed temperature and salinity profiles is done through a Reduced Order Optimal Interpolation (ROOI) scheme. This scheme is implemented using the SOFA 3.0 software (De Mey and Benkiran, 2002) after ad-hoc changes in both the numerical and assimilation aspects which transform the original code into a more computationally efficient scheme suitable to be used for global assimilation. More technical information about the assimilation system can be found in the CIGODAS technical report (Di Pietro and Masina, 2009).

An important feature of this ROOI scheme lies in the multivariate structure of the background error covariance matrix, which spreads the corrections over different parameters. In the present implementation the state vector is defined as the temperature and salinity vector. Bivariate background-error vertical covariances are represented by bivariate EOFs of temperature and salinity. This implies that when, for example, only vertical temperature profiles are assimilated, corrections are applied to salinity as well by the vertical EOFs (Bellucci et al., 2007).

The multivariate EOFs used for assimilating in situ data have been diagnosed from the vertical temperature and salinity profiles provided by the ocean model simulation where no data assimilation was applied, i.e., the CTRL experiment. In order to reduce the problem size and filter out noisy vertical correlations, only the first ten dominant modes are retained.

The analyses are composed of a sequence of assimilation cycles and ocean model integrations (Bellucci et al., 2007). The assimilation time-window is 15 days, and the assimilation increments are applied at once at the beginning of the 8^{th} day of the assimilation cycle. The ocean variables

are computed as daily averages by the ocean model and daily outputs are then processed to produce monthly means of the same variables.

Within our experiments, we have used three different sets of static EOFs:

- V1: EOFs are calculated for different macro sub-regions, each representing different dynamical regimes and are time independent;
- V2: EOFs are calculated for each grid point, and are seasonally dependent . The EOFs are evaluated from horizontally smoothed temperature and salinity fields using a three point radial mean filter;
- V3: EOFs are calculated for each grid point, and are seasonally dependent. The EOFs are evaluated from temperature and salinity fields without horizontal smoothing.

2.3 Observed temperature and salinity profiles

The observed temperature and salinity used in our re-analyses are taken from the EN (ENACT Quality Checked) dataset (Ingleby and Huddleston, 2007). The profiles are obtained primarily from the WORLD OCEAN DATABASE 2005, supplemented using data from other sources: GTSPP from 1990 onwards and the USGODAE Argo Global Data Assembly Centre (GDAC) for Argo data from 1999 onwards. The latest processing of the data were performed for the EU supported project ENSEMBLES. Earlier quality control development and processing were performed for the EU ENACT project (Ingleby and Huddleston, 2007).

Four different releases have been used:

- EN1: this dataset covers the period from 1956 to 2001. An error over the XBTs (erroneous double drop rate-correction) affects this dataset.

- EN2: this dataset covers the period from 1956 to 2001. The error affecting the XBTs in the EN1 release has been removed in this release (EN2_v1a release). For both EN2 and EN1 the quality checked has been performed against Levitus et al., (1998) climatology.

- EN3_v1c : this release covers the period from 1956 to 2006. The quality check adopted in this release has been further refined, mainly adopting a new reference background obtained from objectively analyzed temperature and salinity fields derived from the EN2 dataset.

- EN3_v2a (http://www.metoffice.gov.uk/hadobs/en3) : this release covers the period from 1950 till present, and it is updated monthly. The quality check adopted in this release is the same of EN3 v1c, but the raw data used to produce this dataset has been completely recollected from the original sources (WOD05,GTSPP,ARGO). This release is also supplemented by the Arctic Synoptic Basinwide Oceanography project (ASBO) data . This data set does not implement any kind of time varying XBT corrections. A set of monthly 3D temperature and salinity fields constructed by means of objective analysis of EN3_v2a vertical profile is also delivered each month, and is used in this work.

The EN2, EN3_v1c and EN3_v2a XBT data sets are corrected following the same common procedures, described in Ingleby and Huddleston (2007). This procedure involves the corrections proposed by Hanawa et al. (1995) further corrected for colder water masses (cold water tapering) as proposed in Kizu et al.(2005). The time varying XBT correction proposed by

Wijffels et al. (2008) constitutes a separate and parallel dataset currently based on the EN3_v2a, and which has not been adopted in this study.

3. A set of global ocean re-analyses: skill evaluation

A set of re-analyses produced with the CIGODAS (see Table 1) have been compared with the aim of estimating their differences and their quality. Some of these analyses can be downloaded at http://ddc.cmcc.it:8080/DDCPortal-v3.0/usage.jsp.

Several methods can be used to evaluate the skill of a re-analysis, the most common being comparison with independent observed data or objectively analyzed fields. Since our re-analyses have been produced by using all the available in-situ temperature and salinity observations the availability of independent T and S data was very limited. Nevertheless, even if some data sets are not independent since they have been assimilated into the system, the comparison with such long time-series high-quality observations is an indication of the internal consistency of the system and here we will show the comparison with TOGA-TAO T and S (Section 3.1) and with salinity observations at Bermuda Station (Section 3.2). Furthemore, several diagnostics are performed during the assimilation cycle in order to monitor the analysis. Among the others, the innovation statistics provided by the root mean square (RMS) of the observations before being assimilated and the model background, is an efficient tool for discovering the presence of observations affected by problems and for monitoring the fit of the analysis to the observations. For temperature the results are very similar to those found in Bellucci et al., (2007) and showing a decreasing trend of the RMS of innovations both near the surface and in the subsurface upper ocean. The larger data abundance and coverage of the surface ocean is likely the cause of the faster decrease of the near-surface innovations RMS compared to the sub-surface (not shown).

At both depths the decreasing trends are very similar for the three re-analyses considered (OI3, OI4 and OI5). For salinity (Fig.1) is also evident the effect of the number of observations in reducing the differences between observations and background more near the surface than below. However, for salinity it is possible to detect a clear and large decreasing trend (0.2 psu in 6 years) only after the advent of the Argo profiling floats. It is also interesting to note the effect of the decrease in the observation number on the innovation statistics over the 1990-2000 decade which will be further discussed in the following sections.

The most severe validation is however against independent (i.e. not assimilated) observations, in particular of variables which are not directly corrected by the assimilation method but are modified only by model dynamics after T and S have been assimilated. Here we present some diagnostics against surface and subsurface velocity observations and against sea level data from altimetry. Both of them are quite severe diagnostics for some of the reasons explained in Section 3.3.

3.1 Evaluation against the TOGA-TAO moorings: T and S

We use here the TOGA-TAO moorings monthly temperature and salinity from 1987 to 2006 to evaluate the system skill in representing the upper equatorial thermal and salinity structure and its variability.

Sample time-depth sections of temperature differences between model and TAO data interpolated on the model vertical levels (Fig.2 shows for example the difference on the equator at 165°E) indicate that the assimilation of observed temperature induces a more realistic thermal structure in the Equatorial Pacific, and in particular it improves the vertical gradient at the

thermocline level. The CTRL experiment fails to represent correctly the vertical gradient (Fig. 2 , upper panel), and a large bias located around the thermocline region can be observed. The OI1 experiment (second panel), which uses a time-independent set of EOFs defined over the whole equatorial Pacific belt is able to obtain an improvement by reducing the warm temperature bias in the upper 100m. The OI2 re-analysis which uses new refined EOFs sets and newer releases of observed profiles does not seem to introduce other significant improvements, at least at this location. Similarly, the following changes in EOFs and observations (for example OI5, Fig.2 bottom panel) do not have strong impact on the thermal equatorial structure. However, it might be interesting to notice the reduction of the differences between OI5 and TAO after 2002 which is confirmed also at 140°W on the equator (not shown). We believe that the error decrease might be associated with the advent of Argo more than the change of forcing fluxes from ERA40 to operational products since this last change has no evident beneficial impact on the CTRL at none of the two locations.

In order to give a more quantitative evaluation of the impact of the different EOFs and assimilated observations in the Equatorial Pacific, temperature and salinity Root Mean Squared Differences (RMSD) between TAO, CTRL and ocean re-analyses have been calculated at every TAO location over the same time period 1987-2001. For instance at 140°W (Fig.3, left panel) temperature shows a clear RMSD reduction when OI1 is compared with CTRL at all latitudes but 5°S. A further RMSD reduction is also obtained in OI2 re-analysis (EN2 dataset and EOFs V2), even if we cannot conclude if the improvement with respect to OI1 is due to the different data set or the different EOFs. A larger overall improvement achivied with OI3 can be explained by the better quality of observed data (EN3 vs EN2) considering that the same EOFs of OI2 have been used. On the other hand, a further little improvement in RMSD obtained with OI4 and OI5

re-analyses can be attributed to the new EOFs adopted (V3 vs V2). In summary, the assimilation has a beneficial impact with respect to the CTRL, and the introduction of EN3 has the most significant improving effect as shown by the RMSD averaged over all the TAO locations (Table 2). The RMSD vertical profile for a single buoy at 140°W, 9°N, where the positive impact of assimilation is maximum, shows that the largest improvements are confined between 50-100m at the thermocline depth while are practically indistinguishable in the mixed layer and below the thermocline (Fig.3, right panel). At this location we note the maximum improvement of OI4 with respect to OI3 suggesting that the EOFs calculation without any spatial horizontal filter introduced in OI4 is particularly beneficial in regions of very large horizontal temperature gradients such as the upwelling region north of the equator.

On the other hand, RMSD evaluation using the TAO salinity data over the common period 1988-2001 does not always show a positive impact of the assimilation with respect to the CTRL. For example, the RMSD for the buoys located along the latitudinal transect at 156E (Fig.4, left panel), where the salinity observations are the most abundant, increase for OI2 and OI3 with respect to the CTRL for the majority of latitudes. On the other way, the improvement is evident for OI4 and OI5 at all latitudes with the only exception of the buoys at 2°S and 5°S. Also for the buoys at all the other longitudes it is not possible to draw a general conclusion even if the RMSD averaged over all the TAO locations (Table 2) indicate a slight improvement of OI5 with respect to the CTRL and the other OIs over the period 1988-2001. When the period is extended to 2005 a larger RMSD reduction of the OIs with respect to the CTRL is likely due to the positive impact of the Argo data. The vertical profiles of the RMSD for all the latitudes north of the equator (5°N is shown in Fig.4b) show a general improvement of the OIs with respect to the CTRL in the

upper layer above the pycnocline depth, at about 120m. Below this depth the CTRL is almost always better than the OIs.

3.2 Evaluation of the skill at the Bermuda Station

The assimilation system skill in the North Atlantic has been evaluated using the 1962-2001 Bermuda Station (32N, 64W) time series being the longest available salinity record. We will focus here only on the salinity, being more critical than temperature, and use observed monthly salinity time-depth series. Fig.5 shows that the CTRL is unable to correctly represent the salinity evolution in the upper layers (0-300 m.); though broadly preserving a realistic vertical structure in the lower levels (300-500m). The ocean re-analyses, on the other hand, are able to better reproduce the salinity time variability in the upper levels, but the side effect (mostly for OI2 and OI3) is an increase of salinity in the lower levels. OI1 is apparently less affected by this problem, but it shows a large freshening beginning in 1994 onwards which will be discussed also in the following sections. On the other hand, the latest re-analyses do not show any freshening or salting trends. We think that the very bad quality of salinity in North Atlantic in OI1 is the effect of a mixture of problems due to the EOFs used and the data set assimilated. The V1 EOFs adopted in OI1 are built averaging over large areas (21 regions for the global domain), are not time-dependent and therefore cannot be representative of regions characterized by high mesoscale activity and high frequency variability such as the Gulf Stream region. Furthermore the EN1 data set is affected by an erroneous double drop rate-correction that determines overestimated temperature corrections after 1995 (see Fig. 12) and statistically induces unrealistic salinity corrections particularly evident in the North Atlantic (see Fig. 14). It is also worth noting that the decade 1990-2000 is characterized by a general decrease of salinity

observations that pass the quality checks (observed also at Bermuda) and are assimilated in reality. This poor data decade has an evident detrimental effect on salinity innovations (see Fig.1) since it implies that salinity corrections are mainly based on T-S EOFs.

To quantify the individual skill at Bermuda, the average RMSD over the entire period has been evaluated (Table 2). The values confirm that the best performing re-analyses in reproducing Bermuda Salinity are OI4 and OI5. In general, it is evident that at least at the TOGA-TAO and Bermuda stations the effect of assimilating salinity in a direct or indirect way (when observations are not available) with the ROOI system is not always positive and the reconstruction of the haline state and variability remains a critical problem. Being the EOFs calculated from the model itself, in particular from the CTRL, a probable conclusion is that the locally defined statistics with seasonal dependent variability is not able to translate temperature corrections (that constitutes the large bulk of observations) into realistic salinity corrections. In particular, the salinity corrected through our method at the BERMUDA station seems to be very sensitive to the way in which the EOFs are calculated, showing that the removal of the smoothing of the data around the grid point where they are derived (used in OI4 and OI5) significantly improves the system skill.

3.3 Evaluation of climatological ocean states

The effect of temperature and salinity assimilation at the global scale has been assessed comparing horizontal fields of temperature and salinity differences between climatologies from the re-analyses and objectively-analysed observations (Antonov et al., 2006). In terms of temperature in the upper ocean (fixed level at 95 m) all the re-analysis show a large bias reduction in the northern hemisphere with respect to the CTRL, while in the southern hemisphere

the improvement is not so evident (Fig. 6). The latter feature is clearly related to the data scarcity that affects all releases of the EN datasets in this region until the introduction of the ARGO floats in the early 2000. On the other hand, in the northern hemisphere the Kuroshio Current, the Labrador Current and the Gulf Stream thermal front are better represented, due to the large number of data available. Improvements are also clearly visible in the Northern Pacific, in the Equatorial Region, in the Western Indian Ocean and in the Southern Eastern Atlantic. Overall the biggest improvements with respect to the CTRL are seen in the OI1. The amount and distribution of temperature observations, at least at this depth and for a climatological mean, seems to be the dominant factor, more important than the different treatment of the EOFs. Indeed the OI2, OI3, OI4 and OI5 re-analyses show some very little improvements in further reducing the amplitude of temperature differences from observations. The most noticeable reduction of differences are in the Equatorial Region (in all basins), and along the Gulf Stream path. Due to data scarcity affecting the southern hemisphere for most of the assimilation period in all the re-analyses, the improvement in this region is negligible. On the other hand, the climatology itself used as a reference is much less reliable in the southern hemisphere.

The same differences have been analysed for the salinity in the upper ocean at the same depth. The CTRL and OI1 show that in the North Pacific there is a general reduction of the salinity bias when assimilation is introduced (Fig.7). On the other hand, a large negative bias in the North Atlantic and a positive bias in the Gulf of Mexico are introduced by the assimilation. A more detailed analysis has revealed that OI1 is affected by a drift that progressively reduces the salt content in the upper layers of the water column starting in 1990 in the region south of the Gulf Stream and confined in the uppermost 300m, and by an opposite drift that induces extreme saline

waters in the Gulf of Mexico starting at the beginning of the 70' in the surface layer and continuously propagating to deeper and deeper layers.

In the rest of the globe the assimilation impact on salinity is small and overall difficult to be quantified. Comparison with the OI2 shows that introduction of EN2 dataset (better quality data) and V2 EOFs (seasonal-gridpoint) does not reflect into a reduction of salinity differences with regard to the OI1 experiment (not shown). The OI3 (V2 EOFs, EN3 dataset) on the other hand, shows a better overall result then OI1 in the Pacific and Indian Ocean, but again in the Northern Atlantic and in the Gulf of Mexico there are unexpected large biases that are absent in the CTRL (not shown). The skill improves with the introduction of V3 EOFs in the OI4 and OI5 analyses. While maintaining the good results obtained with the OI3 analysis in the Pacific and Indian basins, in the North Atlantic the differences with Levitus are now minimal (Fig.7, bottom panel). This feature is an evidence that the smoothing applied to the CTRL temperature and salinity fields used to produce the V2 EOFs, and the averaging over large areas adopted to produce the V1 EOFs are introducing in the assimilation of salinity in the Northern Atlantic a large error due to the mixing of different water masses.

3.4 Evaluation against independent data: currents and sea level

The impact of T and S assimilation on the surface currents was studied through comparing monthly means of the zonal component of surface currents against the Ocean Surface Current Analysis-Real Time (OSCAR, Bonjean and Lagerloef (2002)) dataset, which derives surface currents from satellite altimeters and scatterometers (surface vector wind data). An evaluation against subsurface currents is done using the TOGA-TAO mooring monthly zonal velocities. Our assimilation scheme does not correct velocity fields and, therefore, the comparison is a

proxy of how the assimilation of in-situ observations is able to induce a modification in the tropical and sub-tropical upper-ocean circulation. As previously observed also in other applications (see for example Masina et al., 2001) the impact of the assimilation of in-situ data is in general not positive on the ocean currents. The possible reasons are several and not easy to identify. Among them is the inconsistency between the induced corrections in the water masses and the surface wind forcing which might generate the appearance of sporadic currents with deteriorated amplitudes and might be avoided with pressure gradient corrections (Bell et al., 2004). OI schemes where balanced updates of the zonal velocity were implemented in addition to the assimilation of temperature profiles (Burgers et al., 2002) proved to have a beneficial impact on equatorial upper-ocean zonal currents.

The validation against OSCAR data shows that the RMS errors of the re-analyses over the period Oct1992-Dec2001 are always larger with respect to the CTRL even if we note small consistent improvements from OI1 to OI5 confirming the beneficial impact of higher quality assimilated observations and more optimal assimilation strategies. The RMS errors are always larger in the Tropics, especially in the Indian, and smaller polewards (Table 3). On the other hand, area-averaged zonal currents correlations between the OSCAR dataset and the re-analyses (Table 4) are always larger than the correlation with the CTRL, with the only exception of the Tropical Atlantic, suggesting that the temporal variability is slightly better captured when we assimilate T and S in-situ observations. However, the correlations are significantly different from zero at the 95% confidence level only in the Tropical band and in the central North Pacific, with the largest values in the Tropical Pacific (Fig.8a). In the central North Pacific the OI5 zonal currents correlate with OSCAR data better than the CTRL (Fig.8b). Other regions where the assimilation

has a general positive impact on the currents are in the Indian Ocean and the northern tropics in the western Pacific.

The TAO currents at the equator are valuable independent data set to evaluate re-analysis currents even in the subsurface. As expected and for the reasons mentioned above the impact of T and S assimilation on the equatorial currents is, in general, not positive. In Fig.9a the RMSD calculated over the period 1980-1999 (when there is the maximum availability of observations) at 140°W over the uppermost 300 m show that all the re-analyses (with the only exception of OI2) are better than the CTRL from the surface down to about 90 m, approximately the upper bound of the Equatorial Undercurrent. Below this depth the situation is reversed and in terms of amplitude the currents simulated by the CTRL are more similar and more intense (not shown) than those given by the re-analyses. Similar conclusions apply also to the time variability (Fig.9b) that is better captured by the CTRL below the uppermost 100m where the correlation coefficient (statistically significant at 95% confidence level) are about 0.8 for the CTRL and 0.6 for the re-analysis. In the upper layer the correlations are very similar and quite high (above 0.8). At 110°W the RMSD are in general higher for the re-analyses than the CTRL (in the range 0.3-0.5 m/s) in the uppermost 120m and reverse below (in the range 0.1-0.3 m/s).

Altimeter observations represent a completely independent data set since in our re-analyses the sea level is not assimilated. By consequence we can use sea level observations to validate our method even if we should notice that with coarse resolution models as ours sea level comparison is usually a severe diagnostics. The volume conservative model used here explicitly resolves the sea surface height equation which represents the sea level variability only for the incompressible part of the dynamics, so that the globally-averaged variations of sea-level due to the steric effect

are not included. Furthermore, having zeroed the global average of evaporation minus precipitation minus runoff in order to have fresh water budget globally balanced (see Section 2.1) leads our re-analyses to neglect any global trend in the sea-level budget. Being aware of these disadvantageous issues, we assess the impact of temperature and salinity assimilation on the sea level anomaly (SLA) comparing the SLA fields from the CTRL and the re-analyses against monthly maps of SLA produced by Ssalto/Duacs and distributed by Aviso (http://www.aviso.oceanobs.com/duacs). Anomalies have been computed with respect to the 1993-2001 Mean Sea surface Height (MSSH) for all our experiments and with respect to the CNES-CLS09 mean dynamic topography of Rio et al. (2010) - recalibrated for the 1993-2001 period - for Ssalto/Duacs products. In order to simulate the volume conservation of our model, global averages of Ssalto/Duacs monthly SLA have been restored to zero. Even if we do not assimilate altimeter data the assimilation of temperature and salinity profiles changes the density structure and by consequence has an impact on the model sea level. In the global mean the RMS deviations from altimetry data (Fig. 10) have the smallest values for the CTRL even if the negative impact of the assimilation is very small. The differences with respect to the CTRL are always smaller than 0.5 cm for all the re-analyses and therefore not significant if we consider that the instrumental error for the observations is equal to 2-3 cm (Le Traon and Ogor, 1998).

Looking at the RMSE difference between each re-analysis and the CTRL (see Fig.11a for the OI5 case) we can conclude that the CTRL in general performs better in the extra-tropical mesoscale areas, while the assimilation of T and S brings to smaller RMSE in the tropical area (Table 5) and in particular in the tropical Pacific in agreement with Bellucci et al., (2007). OI4 and OI5 are the only experiments which give scores comparable with CTRL in the Gulf Stream region, while OI1 and OI2 are the only ones which give scores comparable with CTRL in the

Antartctic Circumpolar Current (ACC). In terms of variability the assimilation of the in-situ observations induces larger correlations (Table 6) in the Tropics and North Pacific, but smaller in general elsewhere especially in areas characterized by high mesoscale activities (not shown). All the OIs are worst than the CTRL poleward of 40° in both hemispheres (see Fig.11b for the OI5 case). In the ACC region OI1 and OI2 are "less worst" than other OIs. A possible reason is the fact that in the EN3 data set assimilated in OI3, OI4 and OI5 the Levitus et al., (1998) climatology (used as background in EN1 and EN2 data sets) was replaced by a new reference background obtained from objectively analyzed temperature and salinity fields derived from the EN2 dataset. It might be speculated that in regions such as the ACC where the availability of data is very poor the Levitus climatology might be the best choice as reference background. Finally, unlike other experiments, OI1 correlations are much smaller than in the CTRL in Equatorial Atlantic (not shown) suggesting that the higher spatial resolution and the seasonal dependence of the EOFs is beneficial also for the SLA in this region.

4. Heat and Fresh Water content and transport

The ocean heat content (OHC) can be considered as one among the most suitable indicators of climate change since it is less affected by the high-frequency natural variability associated with sea surface temperatures. Similarly for the salt content in the ocean even if salinity is a much more critical variable both because it is not as well observed as temperature and because it is less constrained than temperature by surface fluxes. However, here we analyse the time evolution of both the global averaged heat and freshwater content anomalies integrated over the uppermost 700m from all our re-analyses and the objectively analyzed temperature and salinity fields derived from the EN3 dataset (labelled OA in the plots).

The heat content change time series (Fig. 12) calculated as anomalies with respect to each respective climatology show that all the re-analyses have similar trends, with the exception of OI1 and OI2 from 1994 onwards. In particular, the warming trend of OI1 starting in 1994 is particularly overestimated, but this anomalous behaviour is certainly related to the XBT double correction error affecting the EN1 dataset used in this re-analysis. The CTRL, though broadly following the general trend, has a much reduced variability with respect to the re-analyses, giving a measure of the effect of the assimilation on the estimation of processes at different frequencies likely not simulated by the model because of its coarse resolution, errors in the atmospheric forcing or inaccuracy in representing correctly some physical processes. All the re-analyses show an increase in heat content in the 1970s followed by a decrease in the late 1980s. The "warm period" in the 1970s has been recently recognized as one with enhanced data errors. This notion is now supported by recent studies using corrected XBT observations (Domingues et al., 2008, Levitus et al., 2009). The warming trends over the last decade obtained by the set of our re-analyses (Table 7) differ significantly with respect to Levitus et al., (2009) especially over the most recent period when our estimates are about 50% of the Levitus et al., (2009) positive trend. This last feature is clearly evident both in the North Atlantic and North Pacific Ocean (Fig.12b,c). The differences with respect to Levitus et al., (2009) are smaller on the long-term trend (1962-2001). Nevertheless, it is interesting to note that in all estimates the warming trend doubles if we consider the period 1993-2007 with respect to the longer period 1969-2007. In general our estimates fall in the wide range of values (0.26-0.95 W m^{-2} for the years 1993-2006 in Lyman et al, (2010), see their Table 1) of other recent observation-based estimates of ocean heat content derived by using different methods to treat for example under-sampled areas or to correct biases from XBTs and other instruments (see for example Domingues et al., 2008,

Wijffels et al., 2008 and Ishii and Kimoto, 2009). The reason of the differences has been analyses by Lyman et al (2010) who found out that during the 1993-2008 period the largest source of uncertainty in the OHC estimates comes from the choice of XBT bias correction. In their work Lyman et al. (2010) applied four XBT correction to the same EN3_v2a data set, which is the most recent data set that we assimilated (see OI5 re-analysis), and showed that with the applied corrections they obtain a trend similar to the other estimates. We might conclude that the issue concerning the quality of XBT as well as other instrumental data has not been completely resolved and will continue to affect the estimates derived from the re-analyses. To further understand possible reasons for the underestimation of ocean heat content trends compared with observational estimates we have produced two new experiments, a CTRL without relaxation and another OI5 without relaxation. It is evident (Table 7) that the relaxation drastically reduces a warming trend in the CTRL run that on the long period (1962-2001) more than double that of Levitus et al., (2009). On the other hand, when the data assimilation is introduced the impact of the relaxation is much more reduced. It has no effect at all over the 1969-2007 period and has even the opposite effect on the most recent period (1993-2007), i.e., it increases the warming trend. In summary, we can conclude that the relaxation to climatology applied in our re-analyses cannot be the cause of the underestimation of the heat content warming trends.

A detailed analysis of the regional variability of the estimated trends, their associated uncertainties and the possible causes is beyond the scope of the present study. However, it is interesting to check which are the regions where the biggest differences in the OHC linear trends over the 1958-2006 period are visible if compared to the Levitus et al. (2009) estimates (Fig. 13). Apart from the Antarctic Circumpolar Current region where all estimates from re-analyses as

well as direct observations are significantly affected by data scarcity, the only two regions where the trends from our best re-analysis (OI5) and Levitus et al., (2009) show opposite signs are the equatorial upwelling regions in both the Atlantic and Pacific basins where our re-analysis show a cooling tendency. Possible reasons for this discrepancy might be attributed to different XBTs biases corrections as suggested by Lyman et al. (2010), but it is not clear why we do not find evidence of excessive cooling in our re-analysis in the Equatorial Pacific when we evaluated the system skill against the TAO observations.

The freshwater content anomalies time series is shown in Fig. 14. The main feature is that the CTRL and the OA are relatively stable over the entire period, while each re-analysis starts with a freshwater contents value higher than the mean. All the re-analyses show a negative trend in the 1960-1975 period, while in the following years the freshwater content difference tends to become stable, with the only exception of OI1, which has a strong positive trend starting in 1990 and reflecting the large fresh salinity bias introduced by the assimilation in the North Atlantic (Fig. 14b). This feature is mostly due to an indirect effect of the EN1 XBT error which is generating biased salinity corrections evaluated from biased temperature corrections through the bi-variate EOFS used in the assimilation. In the North Pacific (Fig.14c) the spread of the re-analyses is much smaller and all the experiments seem to follow the observed long-term freshening tendency.

The main conclusion is that the uncertainties affecting the freshwater content derived by the re-analyses are much larger than for the heat content (Davey et al., 2006 and Lee et al., 2009) due to the well known scarcity of salinity observations in the ocean and the inaccuracy of most of the assimilation methods in deriving synthetic salinity corrections from indirect measurements. Even

if all the re-analyses tend to stabilize after about 10 years, it is not possible to detect any kind of correlations among the re-analyses at short time scales and the variability among them is large. However, it is likely that the spread among our re-analyses tends to underestimate uncertainties since it does not sample errors in ocean model, forcing fluxes, or assimilation methods, particularly important for salinity. Our re-analyses sample uncertainty only in covariance settings and observational data sets and indeed the Global Synthesis and Observations Panel (GSOP) intercomparison for freshwater content (Stammer et al., 2010) shows even larger spread.

Other integrated quantities important to assess climate variability and that are particularly difficult or impossible to infer from the present observational network are the ocean heat and salt transports. In Fig. 15 the climatological values for both quantities are shown as a function of latitudes and compared with a sparse selection of estimates from observations which, however, cover a period shorter than the one covered by our re-analyses. The biggest differences in the ocean heat transports are seen in the Northern Hemisphere where the maximum poleward heat transport is in the range between 1.5 and 2.5 PW (Fig. 15, left panel) similarly to the range given by the estimates based on the atmospheric re-analyses from the National Centers for Environmental Prediction–National Center for Atmospheric Research (NCEP–NCAR) and the European Centre for Medium-Range Weather Forecasts (Trenberth and Caron, 2001). The use in the assimilation scheme of bivariate T/S EOFs calculated at each grid-point using unsmoothed model temperature and salinity data is responsible for the most significant changes in the North Atlantic heat transport at 25°N (Table 8) confirming again that the reduced order OI method that we use is quite sensitive to the choice of T/S relationship. In particular, the use of the V3 EOFs in OI4 and OI5 causes a smaller climatological heat transport in the latitudinal band 10-30°N that we found to be related to reduced meridional velocities in the western boundary region north of

the equator up to 40°N (not shown) with respect to the other OIs and the CTRL. An analysis of the vertically integrated heat and fresh water content over the whole water column indicates that the main differences between the re-analyses which use the V1 and V2 EOFs and those which use the V3 EOFs is due to an anomalous positive salinity trend localized in the Caribbean Sea region and the Gulf of Mexico which has been discussed in Section 3.3 in the case of OI1 and that is present also in OI2 and OI3. It can be speculated that this anomalous and local salinification might be the cause of induced anomalous and stronger meridional currents.

The estimates of the fresh water content transports are in very good agreement with the few values derived from observations. (Fig.15, right panel and Table 8) even if they seem to be as sensitive to the choice of the EOFs as the heat transport and in the same areas.

5. Summary and concluding remarks

A global ocean data assimilation system such as the one developed at CMCC provides an important tool to synthesize all available observations into a complete dynamical description of the time-varying ocean and its interaction with the remaining climate system. However, the evaluation of the accuracy of the ocean re-analyses by comparison with observations is a preliminary requisite to assess the values of such products and use them to analyze climate variability especially through derived integrated quantities not directly observable.

In summary, it was shown that assimilation of in-situ temperature and salinity with the CMCC Global Ocean Data Assimilation System is generally beneficial for the ocean thermohaline mean state estimation and its variability. Quality and coverage of assimilated observations are extremely important to produce a high-quality re-analysis. However, it is also true that the

information provided by the re-analyses, such as for example the innovation statistics, are valuable tools which might help to detect errors in the observations and, even more importantly, might help to improve the observing system by identifying observational requirements. Ocean state estimation has a deep need for high-quality ocean data, especially data covering the decades before the 1990s, even if the choice of biases corrections affecting especially the XBTs (but not excluding other instruments) is still an open issue which concerns also the most recent decade. In terms of temperature, we have shown that all our re-analyses give a better estimate with respect to the free OGCM run (i.e. without data assimilation). On the other hand, for salinity the assimilation impact is more sensitive to the quality of observations and EOFs calculation. Indeed our study has shown that a careful choice of the statistics included into the EOFs used for the OI is also critical to obtain good results, especially for salinity which is scarcely observed and indirectly corrected using statistical assumptions. Some of the formulations used to calculate the EOFs have lead, in general, to salinity trends which are not seen in free OGCM runs and likely due to the unrealistic mixing of different water masses. The use of EOFs calculated from the original unsmoothed model data at each grid point removed this problem even if an accurate assessment of the salinity content derived from global ocean re-analyses is still not possible. We have also shown that temperature and salinity assimilation slightly improves the correlation of the zonal surface currents with independent (i.e., not assimilated) data in the tropical band even if is unable to correct the model biases and induce robust and clear improvement of the subsurface velocities at all TAO moorings. In terms of sea level, we have found that, in general, the assimilation of T and S brings to better results in the tropical band, especially in the Pacific, but deteriorates the model in mesoscale areas. At the same time, even if we do not show this aspect, the quality of the re-analyses is highly dependent on the model and the forcing used.

Some of the re-analyses described in this paper are currently utilized in the global ocean re-analysis inter-comparison effort coordinated by the GSOP of the Climate Variability and Predictability (CLIVAR) Program and by the Global Ocean Data Assimilation Experiment (GODAE). The effort aims at the inter-comparison of several re-analysis products provided by different European, American, and Japanese institutions using different models, assimilation schemes and observations (http://www.clivar.org/organization/gsop/synthesis/synthesis.php). Examples and applications of some of these re-analyses with a particular focus on climate research are provided by Lee et al. (2010a) and Stammer et al. (2010). Here we have proposed a similar, although limited inter-comparison using only the re-analyses that we performed with the same model in order to assess the impact of the assimilated observations and some of the parameterizations of the assimilation scheme, independently from the different biases which affect each dynamical ocean model.

We have shown that the estimates of the upper-ocean heat content positive trends given by our re-analyses fall within the range of the most recent observation-based products (Lyman et al., 2010). A similar conclusion cannot be made for salinity content variability which is still too uncertain mainly as a consequence of salinity observation scarcity. Some of the advantages of the availability of global three-dimensional ocean estimates such as the re-analyses are clearly given by the possibility to derive integrated quantities (e.g., transports and fluxes) which cannot be directly observed using neither the present nor any realistic future improvements of the observational network. For example, we have shown that at least for climatological values both the heat and salt transports can be derived by the re-analyses.

A major issue with all data assimilation products such as the one that we presented here is that no formal estimates of uncertainties of the estimated ocean states or derived information are provided. Such uncertainties depend on the observing system, the errors of the ocean model, the atmospheric fluxes, and the assimilation system, which are often not easy to estimate. To increase the value of ocean data assimilation products, much effort is needed to characterize the uncertainties in each re-analysis product and to improve them through more advanced assimilation approaches such as the Kalman Filter or ensemble spread-based approach in 3DVar systems which provides posterior error estimates as part of the re-analysis. However, in the present study the spread among the re-analyses might be taken as an indication of uncertainties (Lee et al 2010b, Stammer et al 2010, Xue et al 2010) due to the different quality of the observations and different assimilation statistics.

Another clear disadvantage of the OI scheme currently used at CMCC and presented here is that the solution is always local and, furthermore, the computational cost of an OI scheme is approximately proportional to the number of observations that are assimilated. In the future this may become an important practical limit for the application of OI schemes, because there is a continuous growth of the number of satellite and in situ observations available for assimilation in oceanographic systems. Global ocean 3D-Var variational assimilation systems (see for example Storto et al., in press), in addition to the possibility of providing global solutions for the re-analysis, have the important advantage that their computational cost mainly depends on the size of the state vector and much less on the number of observations.

Acknowledgement:

The authors wish to thank the Centro Euro-Mediterraneo per i Cambiamenti Climatici for its

financial and scientific support of some of the activities presented in this work. The implementation and the following improvements of the global ocean assimilation system were carried out in the framework of the ENACT (EVK2-CT2001-00117) and ENSEMBLES (GOCE-CT-2003-505539) projects. We wish to thank Dr. A. Bellucci for his effort in this activity during the ENACT project. The authors want to thank the AVISO team for the support in the use of SLA data, Dr. Simon Good (U.K. Met Office) for the support in the use of the EN3 dataset, the TAO Project Office of NOAA/PMEL for letting the authors use the TAO/RAMA/PIRATA dataset, and James Carton and Gennady Chepurin for supplying salinity data from Bermuda station. The OSCAR Project Office of NASA is acknowledged for providing the OSCAR data set. The MyOcean (FP7-SPACE-2007-1) project is feeding some of the most recent developments.

References:

Alessandri, A., Borrelli A., Masina S., Carril A.F., Di Pietro P., Cherchi A., Gualdi S. and Navarra A., 2010. The INGV-CMCC Seasonal Prediction System: Improved Ocean Initial Conditions. Mon. Wea. Rev, Vol. 138, No. 7. 2930–2952.

Antonov, J.I., Locarnini, R.A., Boyer, T.P., Mishonov, A.V., Garcia, H.E., Levitus, S. ,2006. World Ocean Atlas 2005 Volume 2: Salinity. NOAA Atlas NESDIS, 62(2). NOAA. 182 pp.

Balmaseda, M. & Co-Authors, 2010. Role of the Ocean Observing System in an End-to-End Seasonal Forecasting System. In Proceedings of OceanObs'09: Sustained Ocean Observations and Information for Society (Vol. 1), Venice, Italy, 21-25 September 2009, Hall, J., Harrison, D.E. & Stammer, D., Eds., ESA Publication WPP-306, doi:10.5270/OceanObs09.pp.03.

Balmaseda, M., Anderson D., and Vidard A., 2007. Impact of argo on analyses of the global ocean. Geophys. Res. Letters, 34, L16 605, doi:10.1029/2007GL0304452.

Bell, M.J., Martin, M.J., and Nichols, N.K., 2004. Assimilation of data into an ocean model with systematic errors near the equator. Q. J. R. Meteorol. Soc., 130, pp. 873–893.

Bellucci, A., Masina, S., Di Pietro, P., and Navarra, A. 2007. Using temperature-salinity relations in a global ocean implementation of a multivariate data assimilation scheme. Mon. Wea. Rev. Vol. 135, pp. 3785-3807.

Bonjean, F. and Lagerloef, G. S. E., 2002. Diagnostic model and analysis of the surface currents in the Tropical Pacific Ocean. J. Phys. Oceanogr., Vol 32, 2938–2954.

Burgers, G., Balmaseda, M.A., Vossepoel, F.C., Oldenborgh, G.J. van, Leeuwen, P.J. van, 2002. Balanced Ocean-Data Assimilation near the Equator. Journal of Physical Oceanography, Vol. 32, 2509-2519.

Capotondi, A., Wittenberg, A., Masina, S. 2006. Spatial and temporal structure of ENSO in 20th century coupled simulations. Ocean Modelling, Vol. 15, (3-4), 274-298.

Carton, J.A., and Santarelli, A. 2008. Global decadal upper-ocean heat content as viewed in nine analyses. Journal of Climate, Vol. 21, pp.6015-6035.

Carton, J.A., Giese B.S., and Grodsky S.A., 2005. Sea level rise and the warming of the oceans in the Simple Ocean Data Assimilation (SODA) ocean reanalysis. J. Geophys. Res., 110, C09006, doi:10.1029/2004JC002817.

Cherchi, A., Masina, S., Navarra, A., 2008. Impact of extreme CO2 levels on tropical climate: A CGCM study. Climate Dynamics , Vol. 31, pp. 743-758.

Davey, M., and ENACT Partnership, 2006. Multimodel multimethod multi-decadal ocean analyses from the ENACT project. Exchanges, 38**,** 22–25.

De Mey, P., and Benkiran M., 2002. A multivariate reduced-order optimal interpolation method and its application to the Mediterranean basin-scale circulation. Ocean Forecasting: Conceptual Basis and Applications, Pinardi N. and Woods J. D., Eds. Springer Verlag, 281-306.

Di Pietro, P., Masina S., 2009. The CMCC-INGV Global Ocean Data Assimilation System (CIGODAS). CMCC Research Papers, RP0071.

Drbohlav, H.K.L., Gualdi S., Navarra A., 2007. A diagnostic study of the Indian Ocean dipole mode in El Nino and non El-Nino years. Journal Of Climate, Vol. 20, Issue 13, pp. 2961-2977.

Domingues, C. M., Church J. A., White N. J., Gleckler P. J., Wijffels S. E., Barker P. M. and Dunn J. R. 2008. Improved estimates of upper-ocean warming and multi-decadal sea-level rise. Nature, Vol. 453, pp. 1090–1093.

Ganachaud, A., and Wunsch C., 2000. Improved estimates of global ocean circulation, heat transport and mixing from hydrological data. Nature, Vol. 408**,** 453–457.

Hackert, E., Ballabrera-Poy J., Busalacchi A. J., Zhang R.-H., and Murtugudde R., 2007. Comparison between 1997 and 2002 El Niño events: Role of initial state versus forcing, J. Geophys. Res., Vol. 112, C01005.

Halkides, D., and Lee T., 2009. Mechanisms controlling seasonal-to-interannual mixed-layer temperature variability in the southeastern tropical Indian Ocean. J. Geophys. Res., Vol. 114, C02012, doi:10.1029/2008JC004949.

Hanawa, K., Rual, P., Bailey, R., Sy, A., and Szabdos, M., 1995. A new depth-time equation for Sippican or TSK T-7, T-6 and T-4 expendable bathythermographs (XBT). Deep-Sea Research I 42, pp. 1423-1451.

Kizu, S., Yoritaka, H., and Hanawa, K., 2005. A new fall-rate equation for T-S expendable bathythermograph (XBT) by TSK. Journal of Ocenography, 61, pp. 115-121.

Ingleby, B., and Huddleston M., 2007. Quality control of ocean temperature and salinity profiles - historical and real-time data. Journal of Marine Systems, Vol. 65, pp. 158-175.

Ishii, M. & Kimoto M., 2009.Revaluation of historical ocean heat content variations with time-varying XBT and MBT depth bias corrections. J. Oceanogr., Vol. 65, pp. 287–299.

Köhl, A., and Stammer D., 2008a. Decadal sea level changes in the 50-year GECCO ocean synthesis. J. Clim., 21, pp. 1866-1890.

Le Traon, P.-Y. and Ogor F., 1998. ERS-1/2 orbit improvement using TOPEX/POSEIDON: the 2 cm challenge. J. Geophys. Res., 103, 8045-8057.

Lee, T., Awaji T., Balmaseda M., Greiner E., and Stammer D., 2010a. Ocean State Estimation for Climate Research. In: Proceedings of OceanObs'09: Sustained Ocean Observations and Information for Society (Vol. 2). Venice, Italy, 21-25 September 2009, Hall, J., Harrison, D.E. & Stammer, D., Eds., ESA Publication WPP-306.

Lee, T. , Awaji T., Balmaseda M., Ferry N., Fujii Y., Fukumori I., Giese B., Heimbach P., Hohl A., Masina S., Remy E., Rosati A., Schodlok M., Stammer D., and Weaver A. , 2010b. Consistency and fidelity of Indonesian-throughflow total volume transport estimated by 14 ocean data assimilation products. Dynamics of Atmosphere and Ocean, Vol. 50 (2), pp. 201-223.

Lee, T., Awaji, T., Balmaseda, M.A., Greiner, E., and Stammer, D., 2009. Ocean state estimation for climate research. Oceanography,Vol. 22 (3), 160-167.

Levitus, S., Antonov J. I., Boyer T. P.,. Locarnini R. A, Garcia H. E., and. Mishonov A. V, 2009. Global ocean heat content 1955-2008 in light of recently revealed instrumentation problems. Geophys. Res. Lett., Vol. 36, doi:10.1029/2008GL037 155.

Levitus, S., and Co-authors, 1998. World Ocean Database 1998. NOAA Atlas NESDIS 1, 346 pp.

Lyman, J.M, Good S.A., Gouretski V.V, Ishii M., Johnson G.C., Palmer M.P., Smith D.M., Willis J.K., 2010. Robust warming of the global upper ocean. Nature, Vol. 465, pp. 334-337, doi:10.1038/nature09043.

Madec, G., Delecluse P., Imbard I. and Levy C., 1999. OPA 8.1 Ocean General Circulation Model reference manual, Note du Pôle de modélisation, Inst. Pierre-Simon Laplace (IPSL), France, No. 11, 91 pp.

Masina, S., Pinardi N., Navarra A., 2001. A global ocean temperature and altimeter data assimilation system for studies of climate variability. Climate Dynamics, Vol. 17, pp. 687-700.

Masina, S., Di Pietro P., Navarra A., 2004 . Interannual-to-decadal variability of the North Atlantic from an ocean data assimilation system , Climate Dynamics, Vol. 23, pp. 531-546

Navarra, A., Gualdi S., Masina S., Behera S., Luo J.-J, Masson S., Guilyardi E., Delecluse P., Yamagata T., 2008. Atmospheric horizontal resolution affects tropical climate variability in coupled models. Journal of Climate, Vol. 21, pp.730-750.

Pierce, D. W., Barnett T. P., and Latif M., 2000. Connections between the Pacific Ocean tropics and midlatitudes on decadal timescales, Journal of Climate, Vol. 13, pp. 1173–1194

Pohlmann, H., Jungclaus J., Marotzke J., Köhl A. & Stammer D., 2009. Improving Predictability through the Initialization of a Coupled Climate Model with Global Oceanic Reanalysis. Journal of Climate, Vol. 22, pp. 3926 – 3938, doi 10.1175/2009JCLI2535.

Rayner, N. A., Parker D. E., Horton E. B., Folland C. K., Alexander L. V., Rowell D. P., Kent E. C., Kaplan A., 2003. Global analyses of sea surface temperature, sea ice, and night marine air

temperature since the late nineteenth century. Journal of Geophysical Research, Vol. 108, No. D14, 4407.

Reynolds, R. W., 1988. A real-time global surface temperature analysis. Journal of Climate, Vol. 1, pp. 75-86.

Rio, M., Faugere Y., Schaeffer P., Moreaux G., Bourgogne S., Lemoine J.M., Bronner E., Picot N., 2010. The New CNES-CLS09 global Mean Dynamic Topography computed from the combination of GRACE data, altimetry and in-situ measurements. ESA's Living Planet Symposium. Berger, Norway, 28 June-2 July 2010.

Stammer, D. and Co-Authors, 2010. Ocean Information Provided through Ensemble Ocean Syntheses. In: Proceedings of OceanObs'09. Sustained Ocean Observations and Information for Society (Vol. 2). Venice, Italy, 21-25 September 2009, Hall, J., Harrison, D.E. & Stammer, D., Eds., ESA Publication WPP-306.

Storto, A., Dobricic S., Masina S., Di Pietro P., 2010. Assimilating along-track altimetric observations through local hydrostatic adjustments in a global ocean reanalysis system. Mon. Wea. Rev. In Press..

Trenberth, K.E., and Caron J.M., 2001. Estimates of Meridional Atmosphere and Ocean Heat Transports. Journal of Climate, Vol. 14, pp. 3433-3443.

Troccoli, A., and Kallberg P., 2004. Precipitation correction in the ERA-40 reanalysis. ERA-40 Project Rep. Series 13, 6 pp.

Uppala, S., and Co-authors, 2005. The ERA-40 reanalysis. Quart. J. Roy. Meteor. Soc., 131, 2961-3012.

Wijffels, S. E., Willis J., Domingues C.M, Barker P., White N.J., Gronell A., Ridgway K., Church J.A., 2008. Changing expendable bathythermograph fall rates and their impact on estimates of thermosteric sea level rise. Journal of Climate, Vol. 21, pp. 5657–5672 .

Xue, Y., Alves, O., Balmaseda, M., Ferry, N., Good, S., Ishikawa, I., Lee, T., McPhaden, M., Peterson, K. and Rienecker, M., 2010. Ocean State Estimation for Global Ocean Monitoring: ENSO and Beyond ENSO. In *Proceedings of OceanObs'09: Sustained Ocean Observations and Information for Society (Vol. 2),* Venice, Italy, 21-25 September 2009, Hall, J., Harrison, D.E. & Stammer, D., Eds., ESA Publication WPP-306, doi:10.5270/OceanObs09.cwp.95

Zheng, F., Zhu J., and Zhang R.-H., 2007. Impact of altimetry data on ENSO ensemble initializations and predictions, Geophys. Res. Lett., Vol. 34.

Table and Figure Captions

Table 1. Summary of the characteristics of the global ocean re-analyses.

Table 2. RMS differences (psu for salinity and °C for temperature) for CTRL and re-analyses with respect to the Bermuda Station and all the TAO buoys for the indicate periods. The values given for the TAO are RMS differences computed for each single buoy at each different depth independently and then averaged.

Table 3. Surface zonal current RMSE (cm/s) of the re-analyses and the CTRL against OSCAR monthly mean surface currents calculated over the period October 1992 (start of OSCAR availability) - December 2001 (end of the shortest reanalyses). The RMSE are given as area-averages of the values at native model resolution, i.e., the statistics are calculated at each grid point and then averaged over the area with the appropriate weights. The tropical band is between 15°S-15°N.

Table 4. As in Table 3 but for the correlation between monthly mean surface zonal currents of the re-analyses and the CTRL against OSCAR data in the tropical band between 15°S-15°N.

Table 5 Sea-level anomaly RMSE (cm) of the re-analyses and the CTRL against AVISO monthly mean sea-level anomalies. Statistics have been computed for all the experiments for the period January 1993-December 2001. The tropical band is between 15°S-15°N.

Table 6. As in Table 5 but for sea-level anomaly correlation of the re-analyses and the CTRL against AVISO monthly mean sea-level anomalies.

Table 7. Linear trend of heat content over 700 m (J/yr *10^22) for Levitus et al, (2009), the re-analyses and the CTRL over different periods. The linear trend has been evaluated as the angular coefficient of a linear fit (robust fit with 95% confidence intervals) applied to a time series of yearly mean values. The yearly means was chosen to be consistent with the Levitus et al. (2009) dataset of annual means. The different fit technique explains the departure of Levitus et al., 2009 given in this table, from what is reported in Lyman et al. 2010

Table 8 Heat transport (PW) and Fresh water transport (Sv) at different latitudes and averaged in the global (GL), in the Indo-Pacific (IND-PAC) basin and Atlantic (ATL) basin for the observations (Ganachaud & Wunsch (2000) and Wijffels et al. (2001)) , the estimates based on the atmospheric reanalyses NCEP–NCAR and ECMWF (Trenberth and Caron, 2001), the CTRL and the reanalyses.

Figure 1. Time series of the globally averaged RMS of salinity (psu) innovations (observation-background) near the surface (continuous line) and at 160m (dashed line) for OI3, OI4 and OI5 (upper panel). A 12-month running mean has been applied to the time series of values representing averages over an assimilation cycle. A similar running mean is applied to the distribution in time of the globally averaged number of observations (bottom panel).

Figure2. Temperature differences (°C) depth-time series between the global re-analyses and TAO moorings located at equator, 165 E.

Figure 3. RMS differences (°C) between temperature TAO observations and temperature from the re-analyses in Table 1 at 140°W and various latitudes (a) and vertical profile of RMS differences at 9°N (b).

Figure 4. RMS differences (psu) between salinity TAO observations and salinity from the re-analyses in Table 1 at 156°E and various latitudes (a) and vertical profile of RMS differences at 5°N (b).

Figure 5: Salinity (psu) depth-time series at Bermuda Station (1962-2001) for observations, CTRL and re-analyses.

Figure 6: Climatological temperature differences (°C) at 95 m depth between CTRL (a), OI1 (b), OI5 (c) and Levitus, respectively.

Figure 7: Climatological salinity differences (psu) at 95 m depth between CTRL (a), OI1 (b), OI5 (c) and Levitus, respectively.

Figure 8: Correlation between monthly mean surface zonal currents of the OI5 re-analyses and OSCAR data from October 1992 to December 2001 (a) and difference between correlations of OI5 and CTRL with respect to OSCAR data (b). In (b) positive (negative) values indicate a better (worse) fit of the OI5 to observations.

Figure 9: RMS differences (m/s) between TAO zonal current observations and the re-analyses in Table 1 at 140°W at the equator (a) and correlation coefficient over the period 1980-1999 at the same location (b).

Figure 10: Globally averaged RMS differences (cm) between SLA observations and the re-analyses in Table 1 over the period January 1993- December 2001.

Figure 11: Difference between RMS errors of monthly mean sea level anomaly (cm) of the OI5 re-analyses and CTRL with respect to observations over the period January 1993 - December 2008 (a). (b) Same as in (a) but for correlations. Negative (positive) values indicate a better (worse) fit of the OI5 to observations in (a) and viceversa in (b).

Figure 12: Heat content (0-700 m) time series (10^{22} Joule) calculated as anomalies with respect to each climatology for the global ocean (a), North Atlantic (b) and North Pacific (c).

Figure 13: Longitude-latitude plots of annual trends of heat content (0-700 m) (10^7 Watt/m^2) for observations (Levitus et al., 2009) (a) and OI5 re-analysis (b).

Figure 14: Fresh-water content (0-700 m) time series (m) calculated as anomalies with respect to each climatology for the global ocean (a), North Atlantic (b) and North Pacific (c).

Figure 15: Climatological global heat transport (PW) (a) and fresh-water transport (SV) (b).

Table 1.

Experiment	Period	Forcing	Assim Data	EOF Set
CTRL	1962-2006	ERA40, ECMWF	--	--
OI1	1962-2001	ERA40	EN1	V1
OI2	1962-2001	ERA40	EN2	V2
OI3	1962-2006	ERA40, ECMWF	EN3_v1c	V2
OI4	1962-2006	ERA40, ECMWF	EN3_v1c	V3
OI5	1962-2009	ERA40, ECMWF	EN3_v2a	V3

Table 2

	Ctrl	OI1	OI2	OI3	OI4	OI5
Bermuda (salinity, 1962-2001)	0.18	0.27	0.20	0.19	0.11	0.11
Tao (salinity, 1988-2001)	0.24	0.23	0.24	0.23	0.24	0.22
Tao (salinity, 1988-2005)	0.22			0.18	0.18	0.17
Tao (temperature, 1987-2001)	0.86	0.62	0.56	0.46	0.44	0.44
Tao (temperature, 1987-2005)	0.82			0.45	0.43	0.43

Table 3

	CTRL	OI1	OI2	OI3	OI4	OI5
GLOBAL	8.34	8.44	8.46	8.43	8.43	8.41
TROPICS	12.97	13.20	13.27	13.20	13.16	13.13
TROPICAL PAC	13.13	13.28	13.43	13.28	13.21	13.18
TROPICAL ATL	10.26	10.95	10.71	11.01	11.04	10.95
TROPICAL IND	15.26	15.35	15.46	15.30	15.27	15.29

Table 4

	CTRL	OI1	OI2	OI3	OI4	OI5
TROPICS	0.256	0.260	0.259	0.262	0.262	0.263
TROPICAL PAC	0.300	0.307	0.301	0.301	0.306	0.307
TROPICAL ATL	0.172	0.135	0.160	0.157	0.156	0.156
TROPICAL IND	0.196	0.211	0.208	0.212	0.210	0.213

Table 5

	CTRL	OI1	OI2	OI3	OI4	OI5
GLOBAL	5.43	5.58	5.63	5.70	5.63	5.60
SOUTHERN EXTRA-TROPICS	6.14	6.19	6.30	6.45	6.46	6.45
TROPICS	3.74	3.72	3.63	3.60	3.55	3.54
NORTHERN EXTRA-TROPICS	6.28	6.76	6.90	6.93	6.71	6.66

Table 6.

	CTRL	OI1	OI2	OI3	OI4	OI5
GLOBAL	0.608	0.590	0.583	0.575	0.578	0.582
SOUTHERN EXTRA-TROPICS	0.466	0.458	0.439	0.419	0.419	0.421
TROPICS	0.822	0.811	0.823	0.825	0.829	0.831
NORTHERN EXTRA-TROPICS	0.587	0.547	0.536	0.534	0.544	0.550

Table 7

	1962-2001	1969-2007	1993-2007
Levitus et al. (2009)	0.25 ± 0.02	0.37 ± 0.03	0.79 ± 0.08
EN3_v2a objan	0.18 ± 0.04	0.14 ± 0.04	0.42 ± 0.08
OI1	0.33 ± 0.05		
OI2	0.22 ± 0.04		
OI3	0.15 ± 0.03		
OI4	0.18 ± 0.04		
OI5	0.16 ± 0.03	0.18 ± 0.03	0.42 ± 0.07
OI5 no-relax	0.27 ± 0.04	0.19 ± 0.04	0.30 ± 0.08
CTRL	0.15 ± 0.02	0.13 ± 0.02	0.38 ± 0.04
CTRL no-relax	0.57 ± 0.02	0.59 ± 0.02	0.85 ± 0.04

Table 8

	GL 25N (PW)	GL 20S (PW)	IND-PAC 25N (PW)	ATL 25N (PW)	GL FW 30S (Sv)	GL FW 25N (Sv)
OBS	1.80±0.30	-0.80±0.60	0.50±0.25	1.30±0.25	0.7±0.3	-0.3±0.3
NCEP	1.78±0.22	-1.01±0.32	0.63±0.17	1.15±0.14		
ECMWF	1.29±0.22	-1.33±0.32	0.44±0.17	0.85±0.14		
CTRL	1.36	-0.86	0.57	0.79	0.73	-0.24
OI1	1.77	-0.84	0.68	1.09	0.76	-0.40
OI2	2.01	-0.67	0.61	1.40	0.85	-0.64
OI3	1.97	-0.77	0.64	1.33	0.83	-0.65
OI4	1.18	-0.75	0.51	0.67	0.77	-0.32
OI5	1.16	-0.75	0.51	0.65	0.78	-0.31

Figure
Click here to download high resolution image

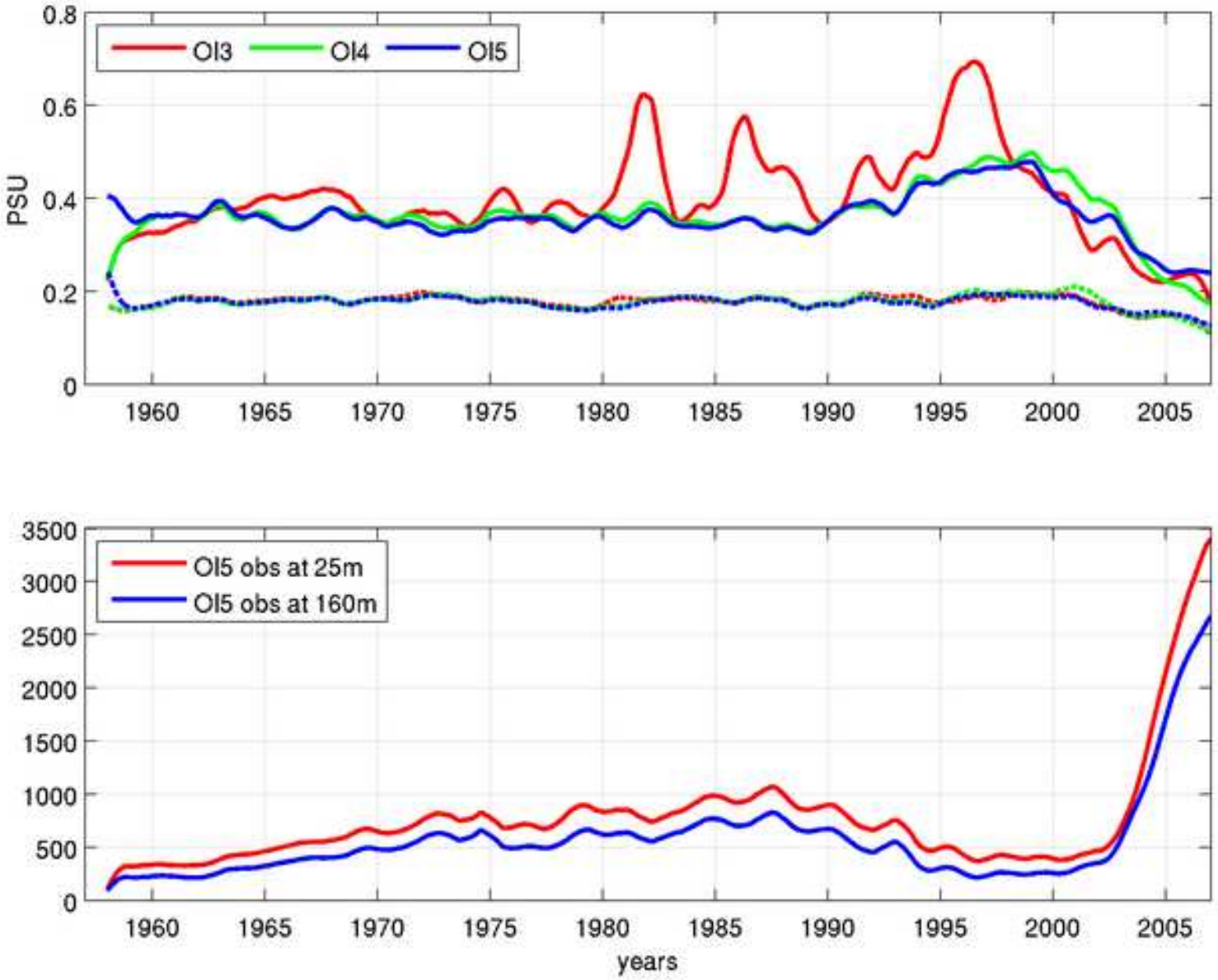

Figure
Click here to download high resolution image

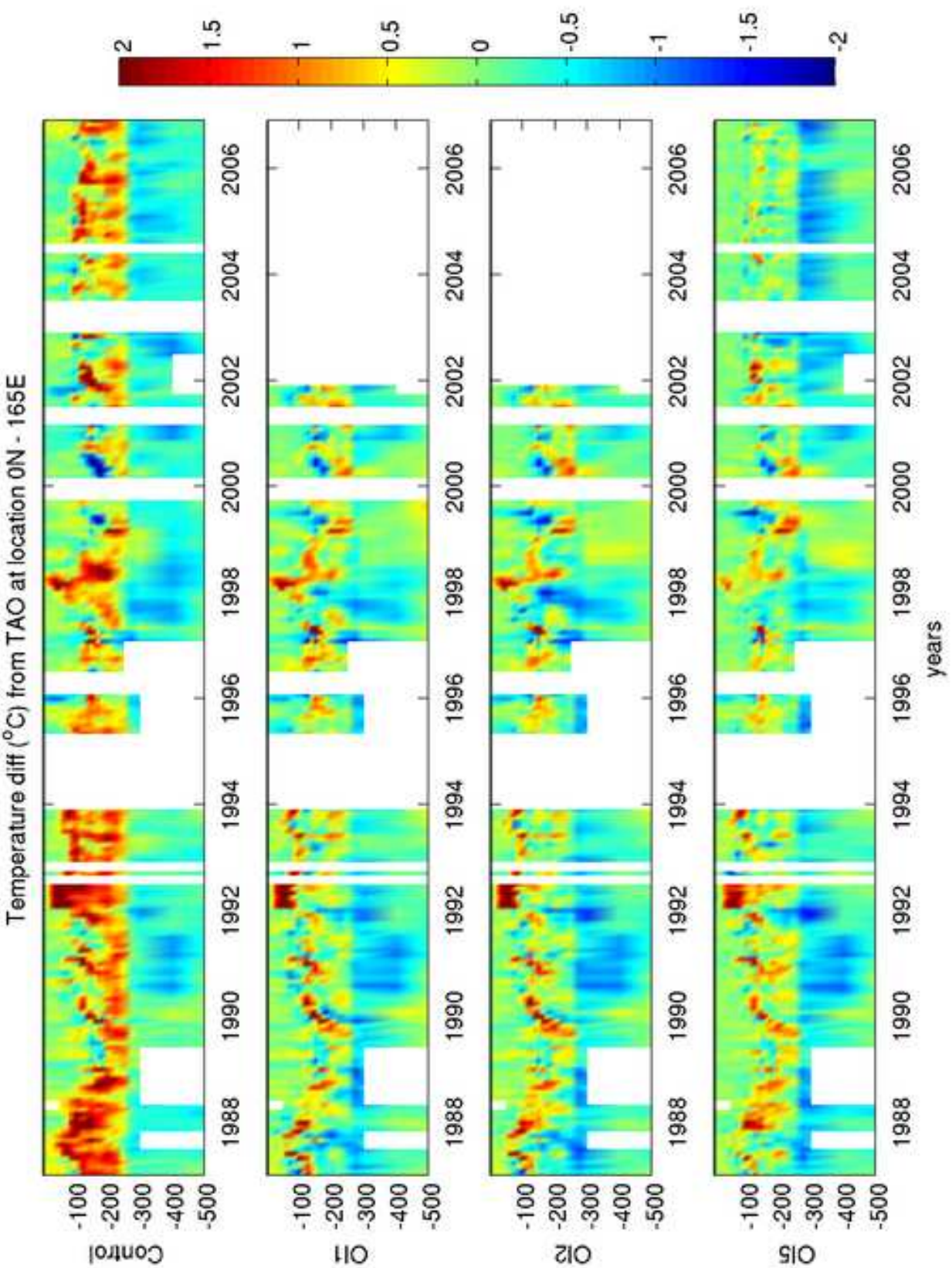

Figure
Click here to download high resolution image

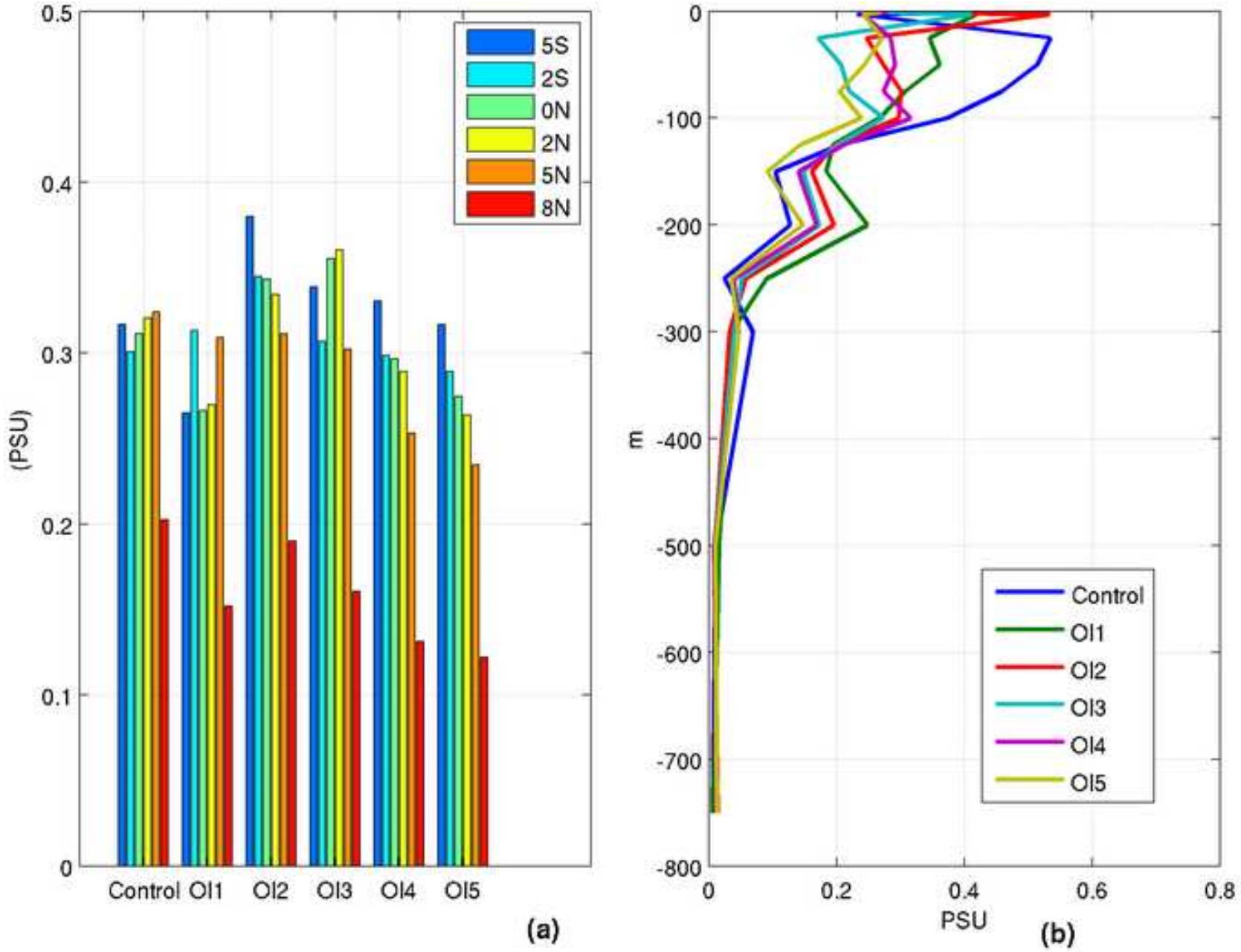

Figure

Click here to download high resolution image

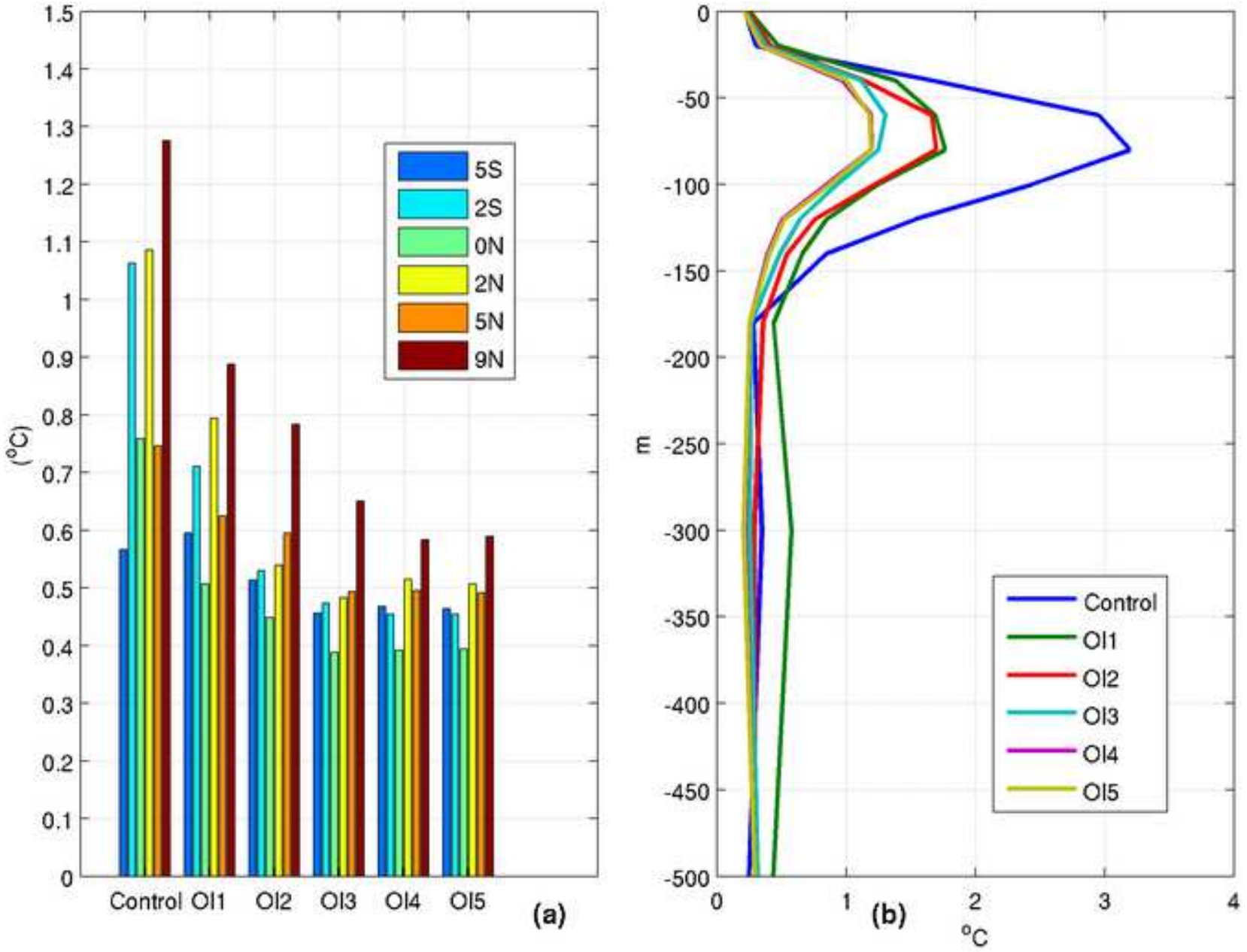

Figure
Click here to download high resolution image

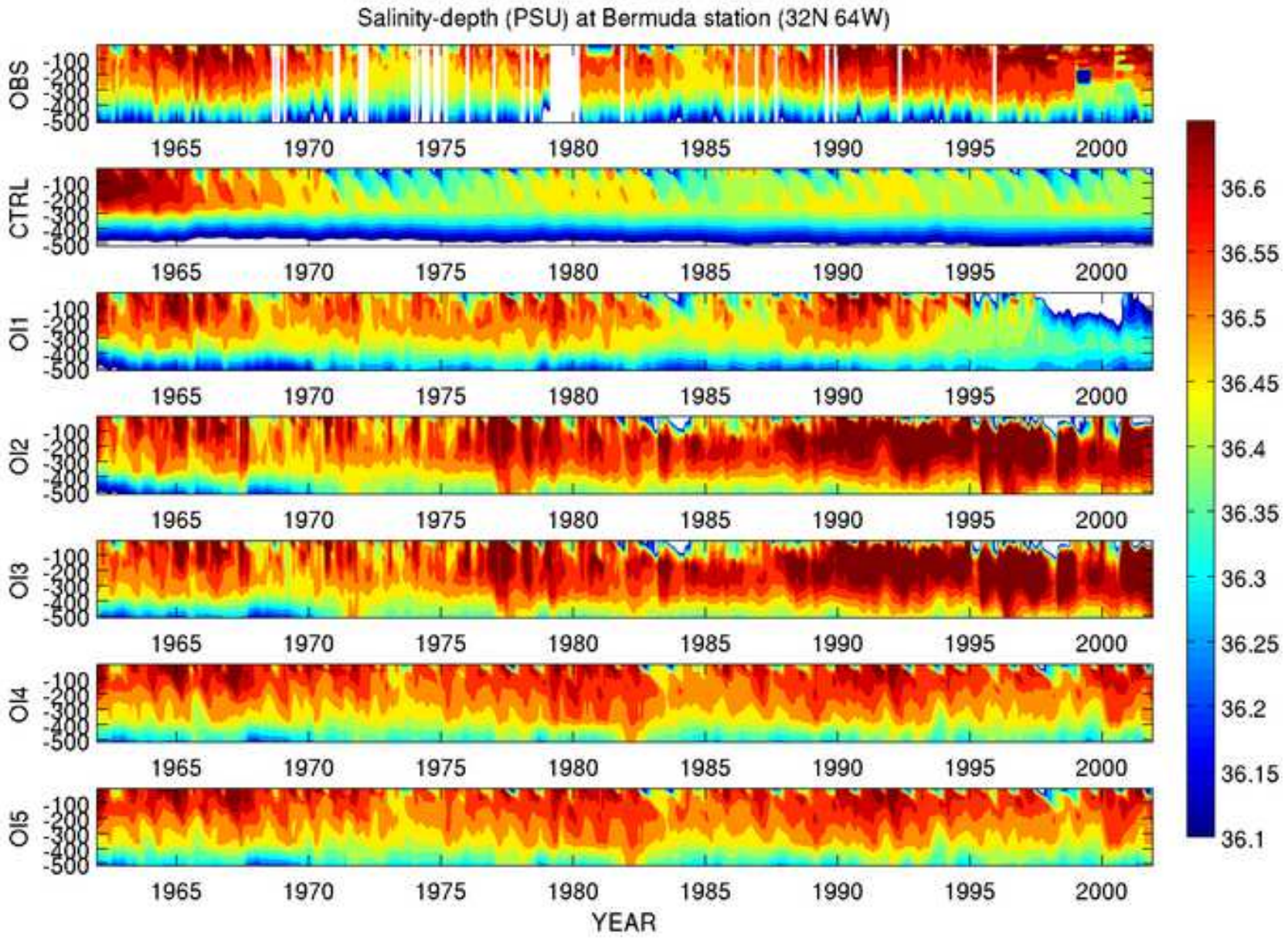

Figure
Click here to download high resolution image

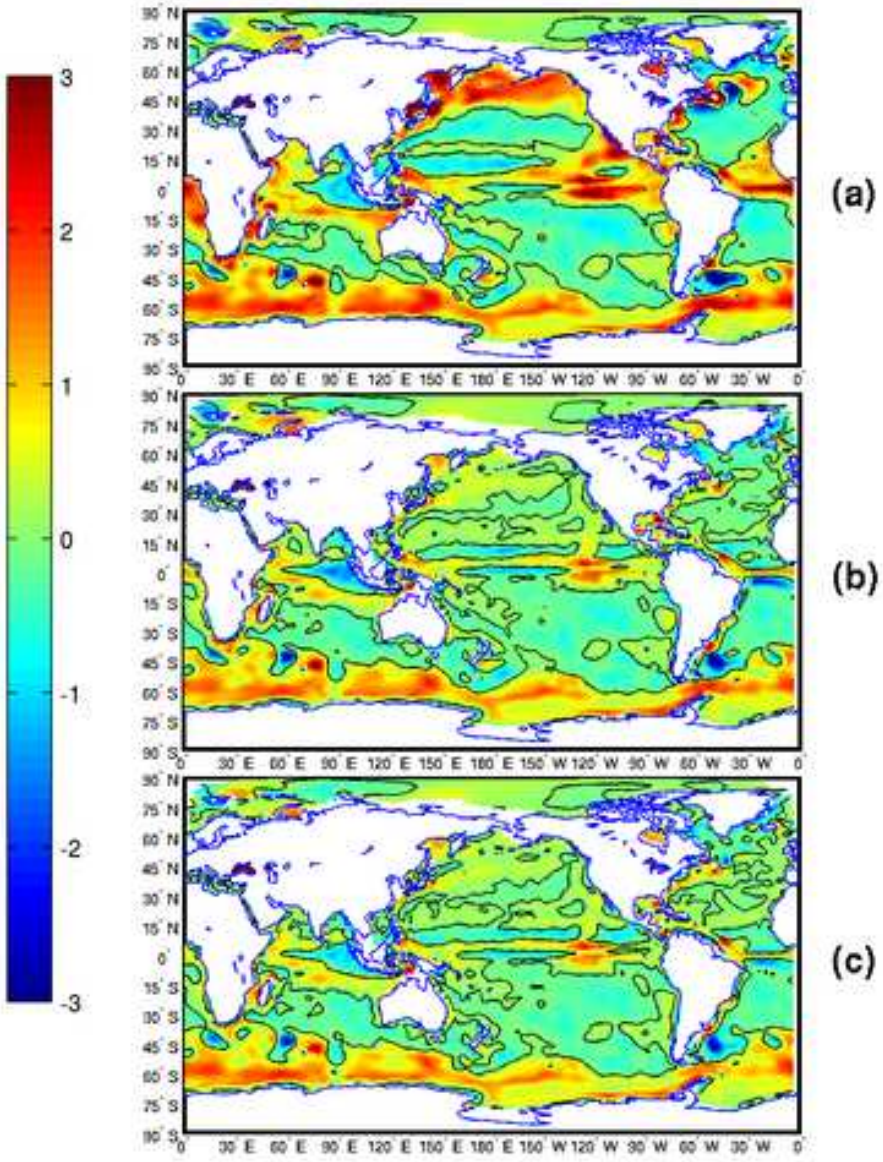

Figure
Click here to download high resolution image

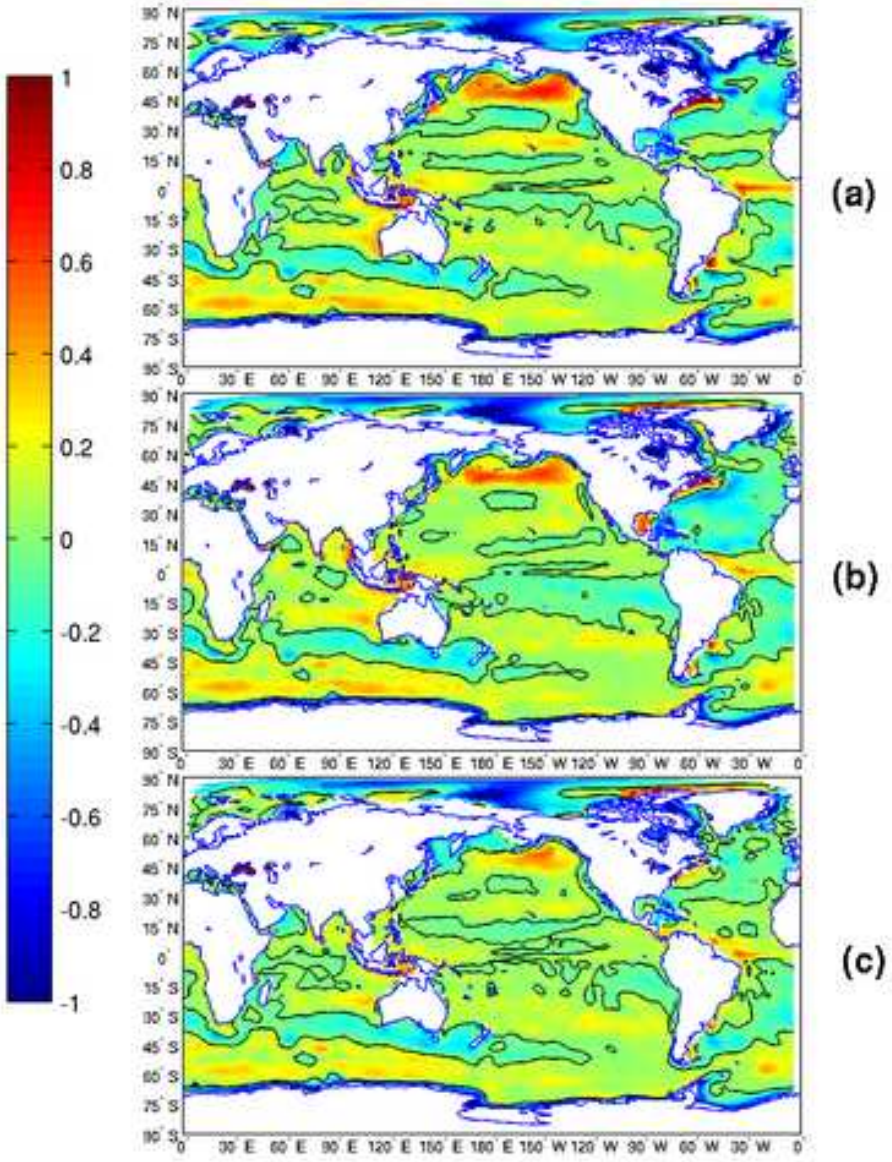

Figure
Click here to download high resolution image

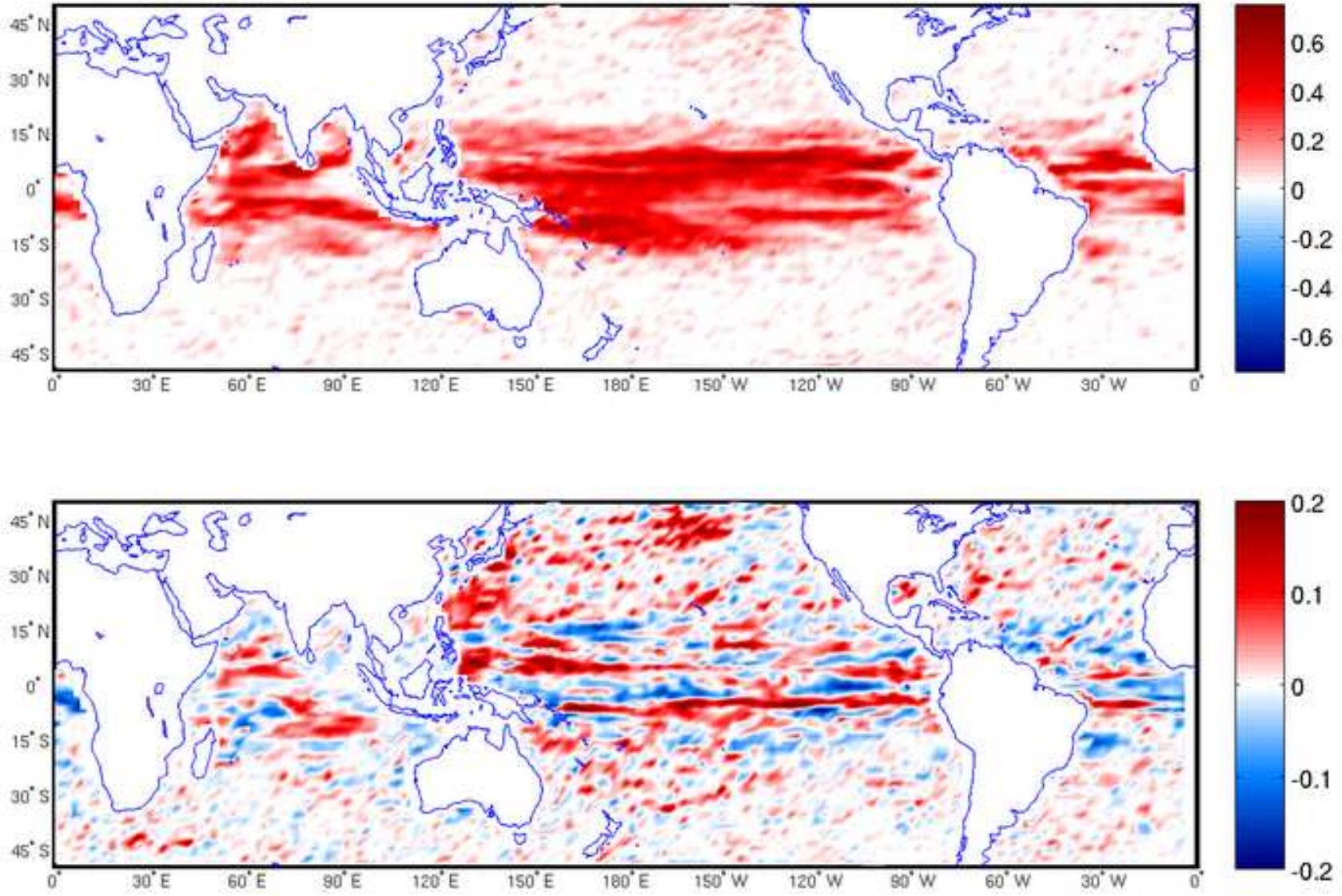

Figure

Click here to download high resolution image

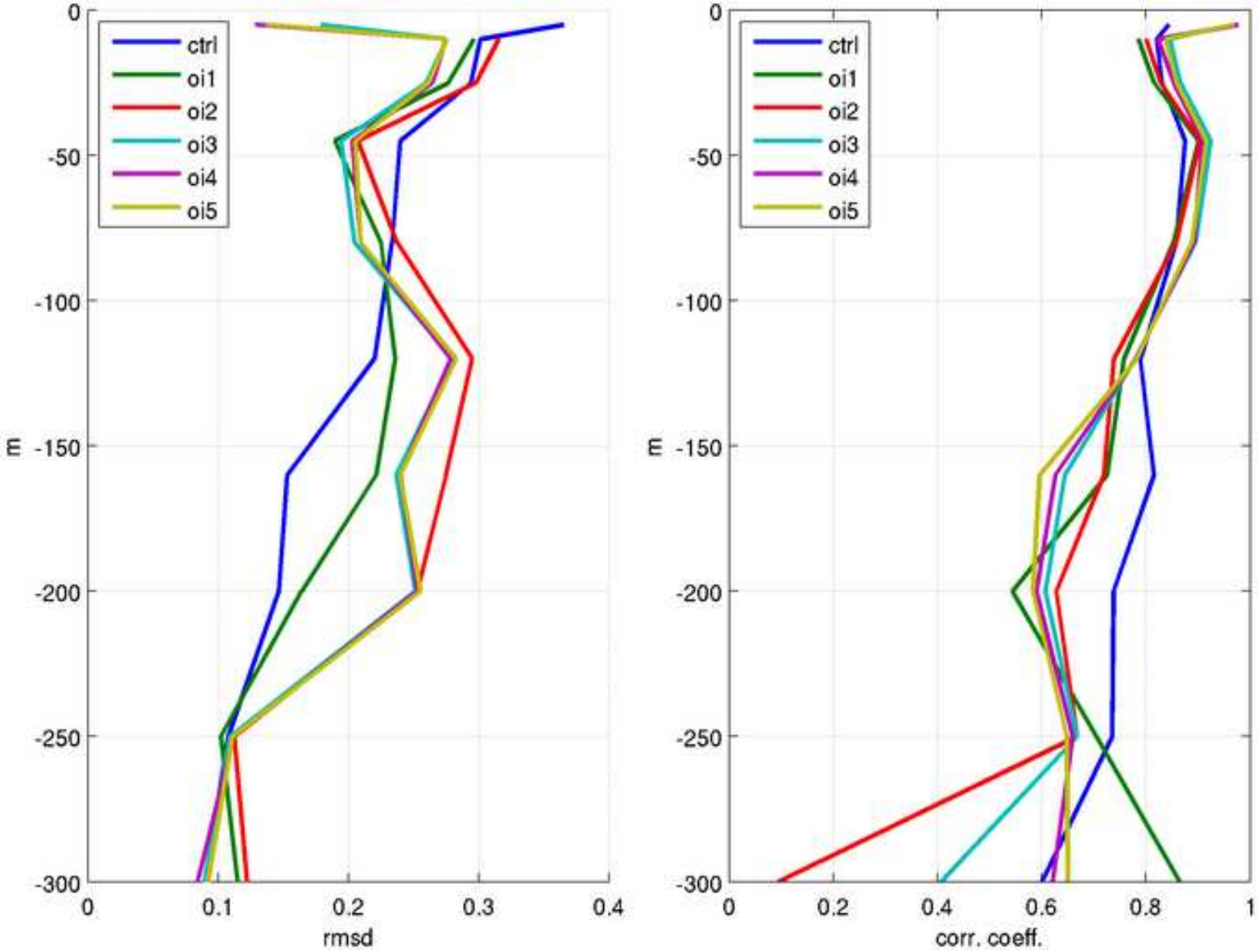

Figure
Click here to download high resolution image

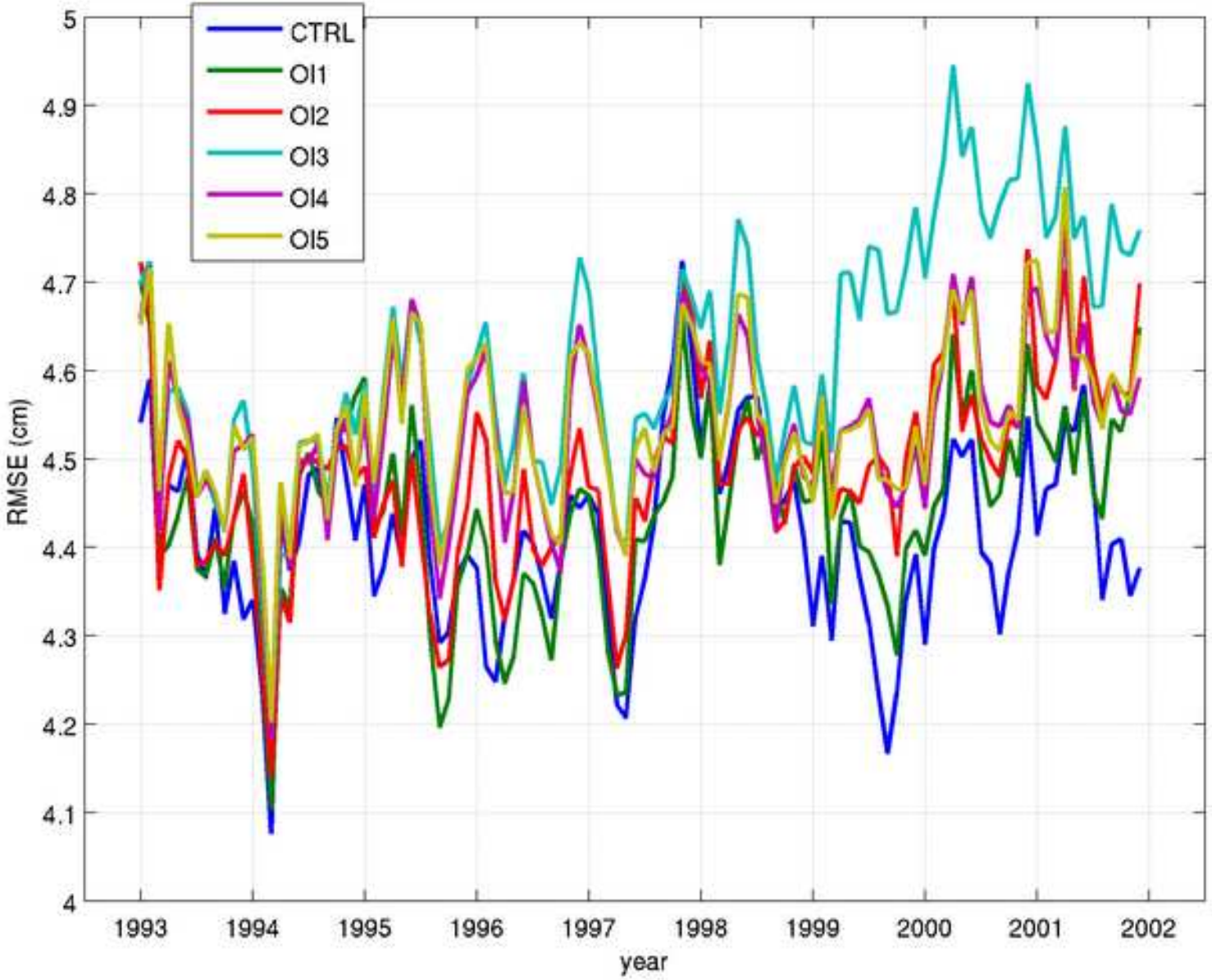

Figure
Click here to download high resolution image

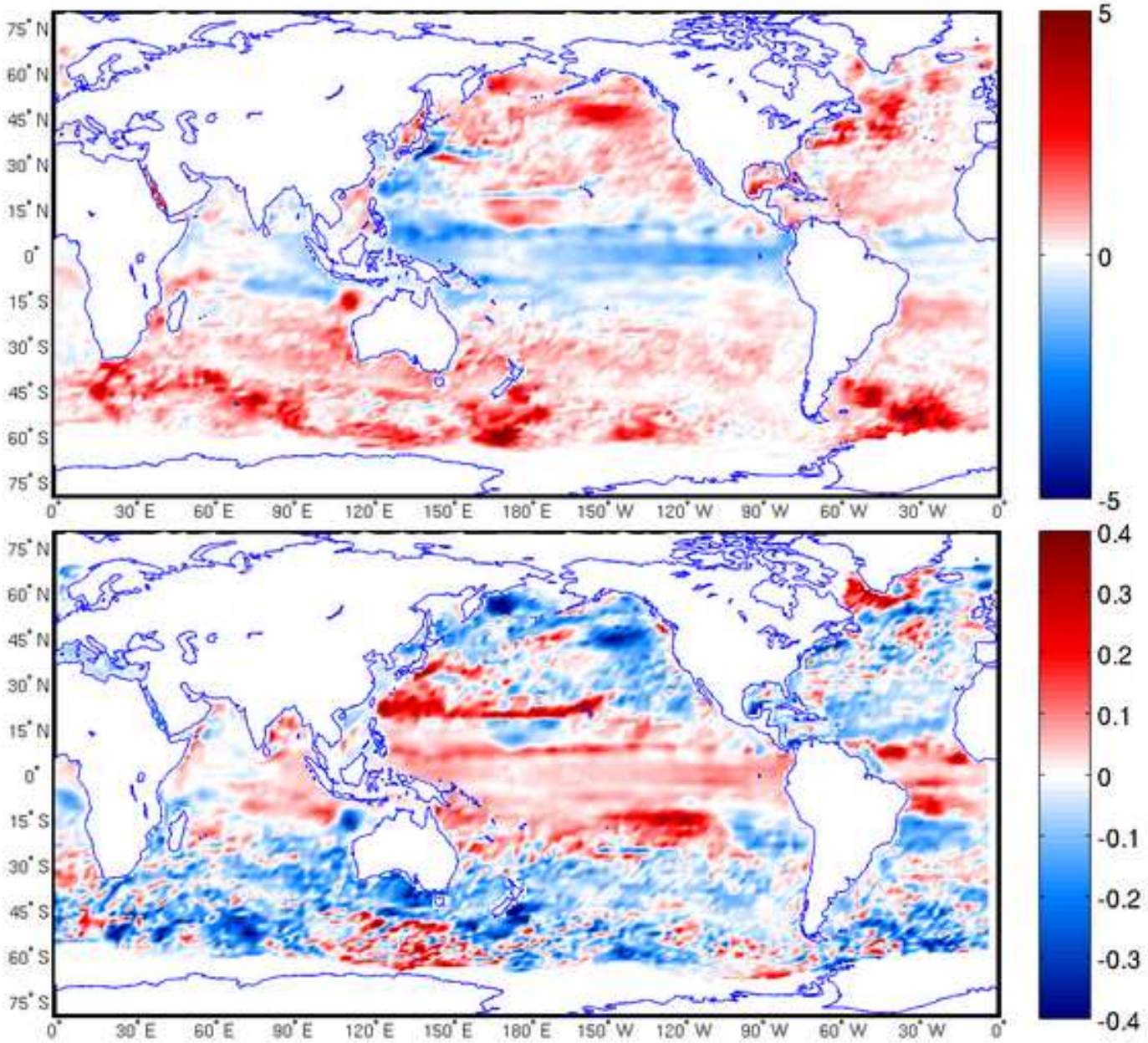

Figure
Click here to download high resolution image

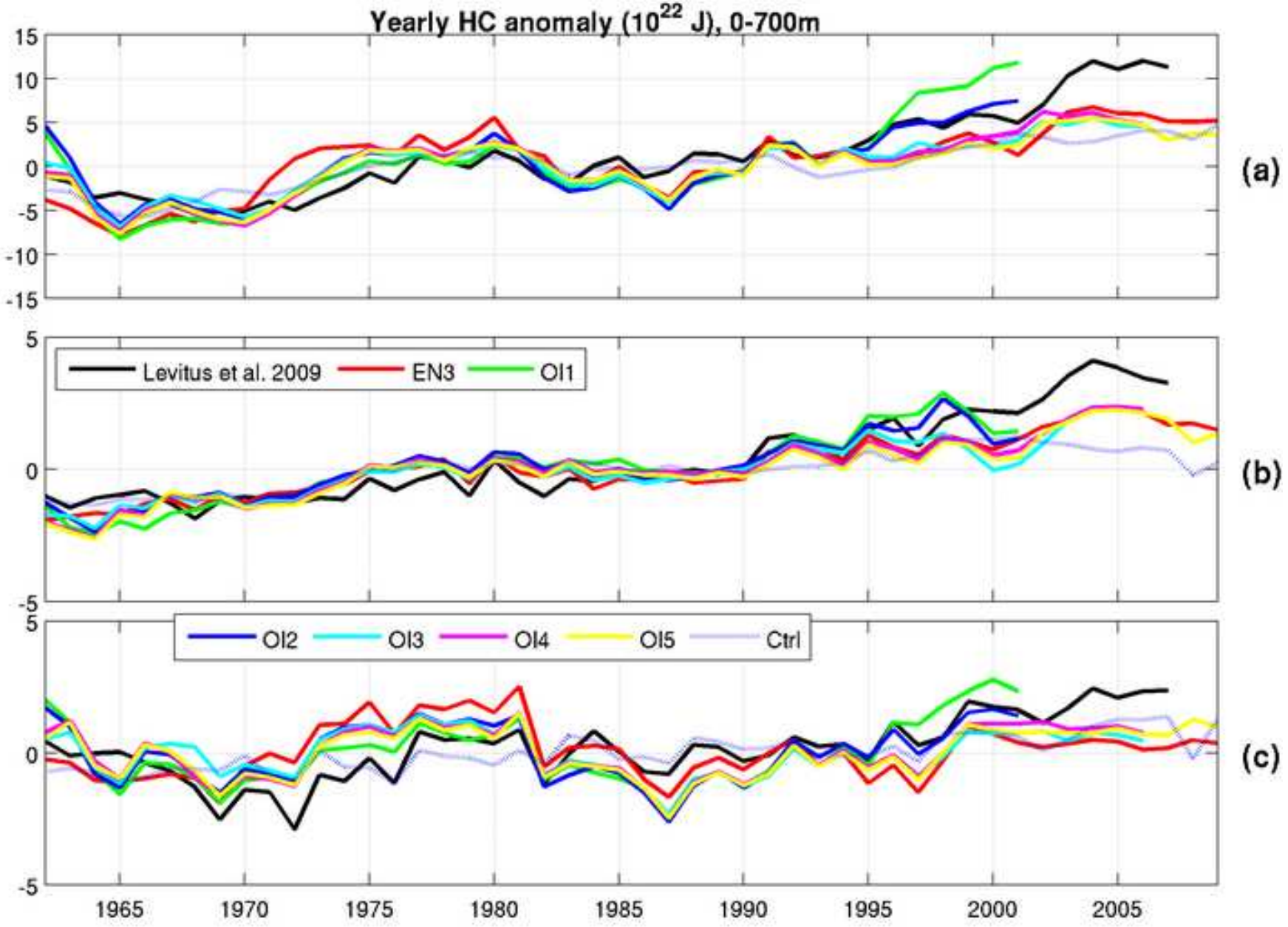

Figure
Click here to download high resolution image

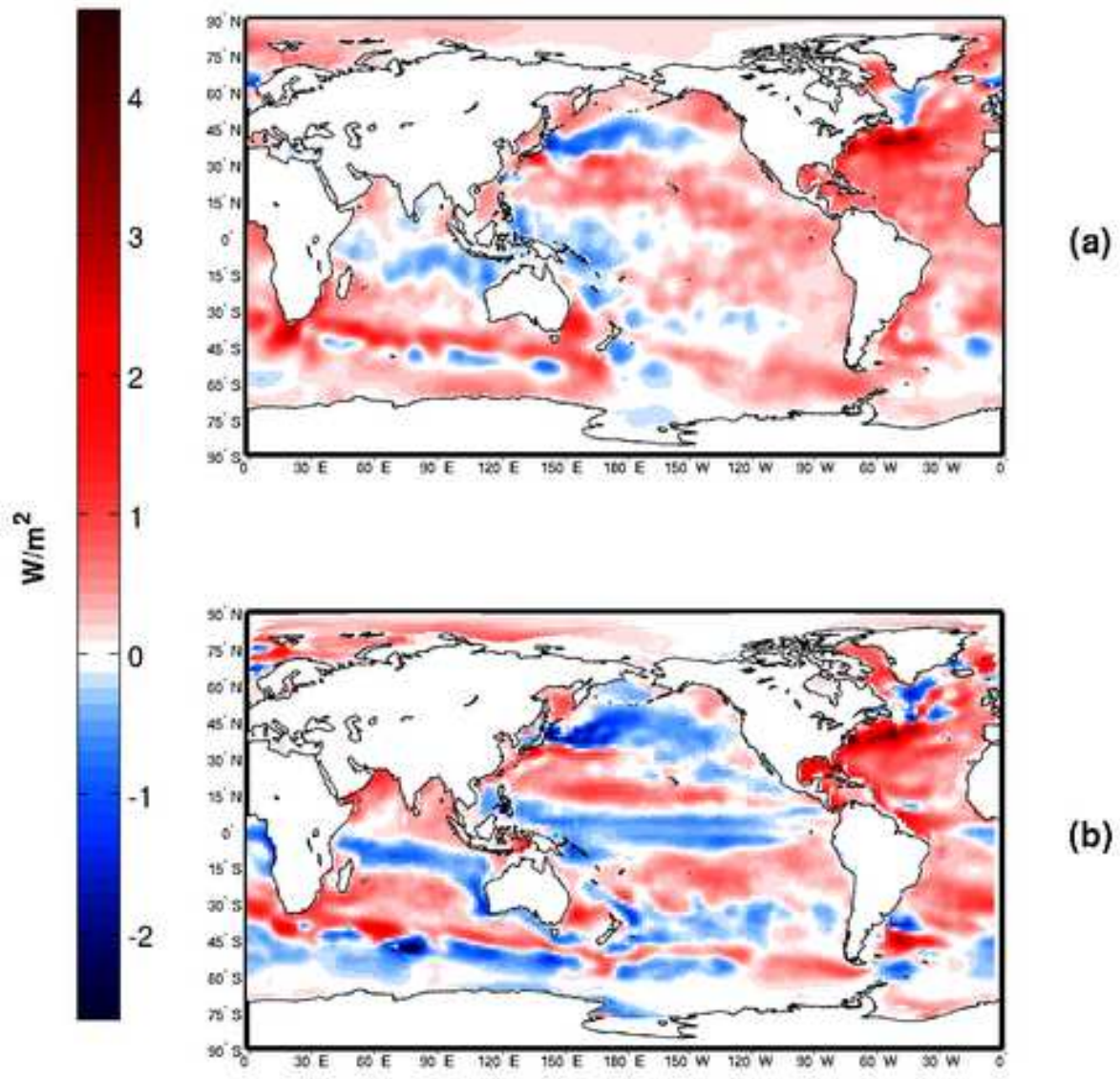

Figure
Click here to download high resolution image

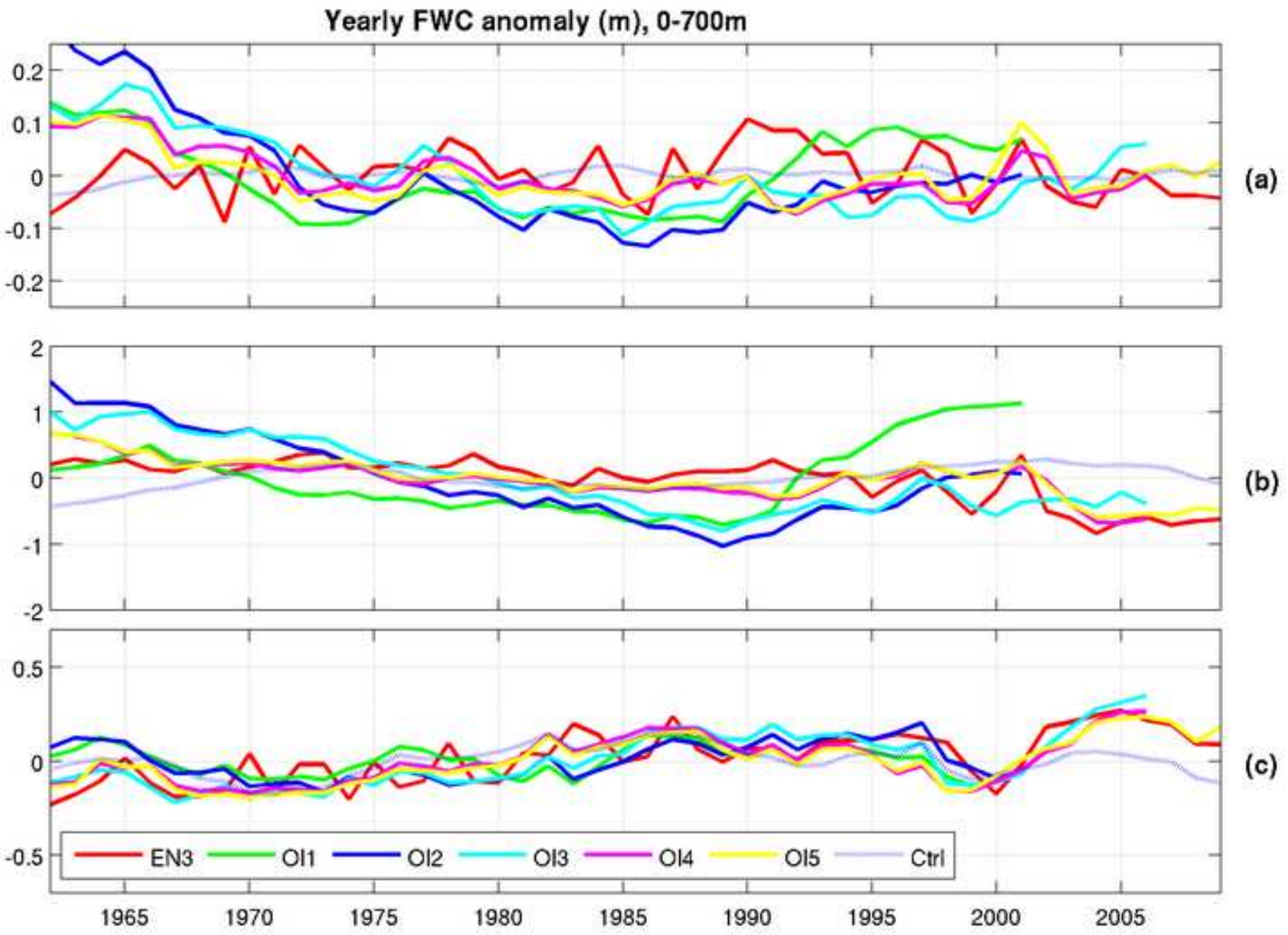

Figure
Click here to download high resolution image